Isoindoline scaffold-based dual inhibitors of HDAC6 and HSP90 suppressing the growth of lung cancer *in vitro* and *in vivo*

Ritu Ojha, Kunal Nepali, Chun-Han Chen, Kuo-Hsiang Chuang, Tung-Yun Wu, Tony Eight Lin, Kai-Cheng Hsu, Min-Wu Chao, Mei-Jung Lai, Mei-Hsiang Lin, Han-Li Huang, Chao-Di Chang, Shiow-Lin Pan, Mei-Chuan Chen, Jing-Ping Liou

PII: S0223-5234(20)30053-2

DOI: https://doi.org/10.1016/j.ejmech.2020.112086

Reference: EJMECH 112086

To appear in: *European Journal of Medicinal Chemistry*

Received Date: 11 November 2019

Revised Date: 18 January 2020

Accepted Date: 20 January 2020

Please cite this article as: R. Ojha, K. Nepali, C.-H. Chen, K.-H. Chuang, T.-Y. Wu, T.E. Lin, K.-C. Hsu, M.-W. Chao, M.-J. Lai, M.-H. Lin, H.-L. Huang, C.-D. Chang, S.-L. Pan, M.-C. Chen, J.-P. Liou, Isoindoline scaffold-based dual inhibitors of HDAC6 and HSP90 suppressing the growth of lung cancer *in vitro* and *in vivo*, *European Journal of Medicinal Chemistry* (2020), doi: https://doi.org/10.1016/j.ejmech.2020.112086.

Graphical abstract

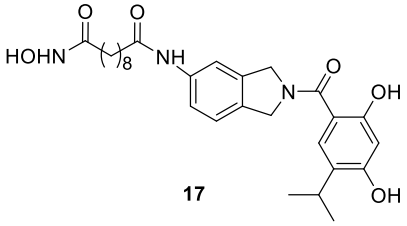

17

GI_{50} = 0.52 μM (H1975); 0.76 μM (A549)
IC_{50} = 46.8 nM (HSP90); 4.32 nM (HDAC6)

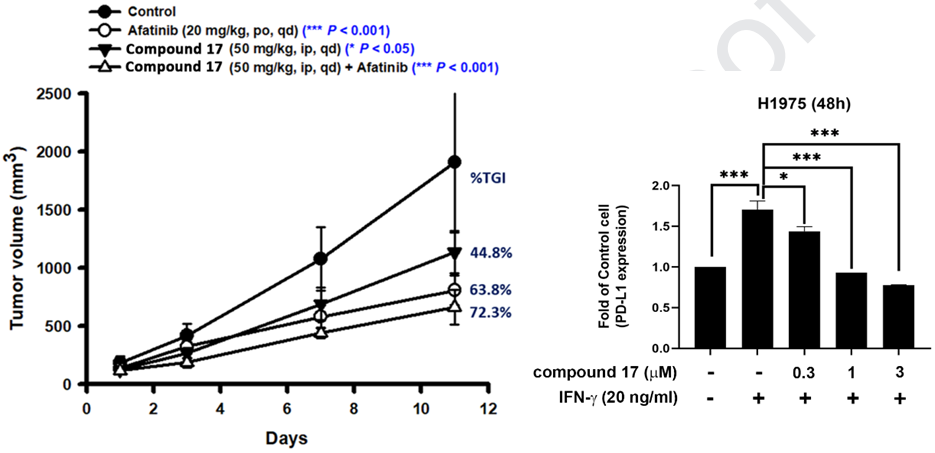

Compound **17** downregulated PD-L1 expression in INF-γ treated H1975 lung cancer cells. Compound **17** in combination with afatinib enhanced antitumor efficacy.

Revised manuscript for Article

Isoindoline scaffold-based dual inhibitors of HDAC6 and HSP90 suppressing the growth of lung cancer *in vitro* and *in vivo*

Ritu Ojha,[a,1] Kunal Nepali,[a,1] Chun-Han Chen,[f] Kuo-Hsiang Chuang,[c,b] Tung-Yun Wu,[b] Tony Eight Lin,[d] Kai-Cheng Hsu,[d] Min-Wu Chao,[d] Mei-Jung Lai,[e] Mei-Hsiang Lin,[a] Han-Li Huang,[e] Chao-Di Chang,[g] Shiow-Lin Pan,[d,g] Mei-Chuan Chen,[b,h,*] Jing-Ping Liou [*,a,e,g]

[1]These authors contributed equally to this work

*To whom correspondence should be addressed. M. C. Chen: (Phone) 886-2-7361661 ext 6184; (e-mail) mcchen1250@tmu.edu.tw; J. P. Liou: (Phone) 886-2-2736-1661 ext 6130; (e-mail) jpl@tmu.edu.tw

[a] *School of Pharmacy, College of Pharmacy, Taipei Medical University.*

[b] *Ph.D. Program in Clinical Drug Development of Herbal Medicine, College of Pharmacy, Taipei Medical University.*

[c] *Graduate Institute of Pharmacognosy, Taipei Medical University.*

[d] *Graduate Institute of Cancer Molecular Biology and Drug Discovery, College of Medical Science and Technology, Taipei Medical University.*

[e] *TMU Biomedical Commercialization Center, Taipei Medical University.*

[f] *Department of Pharmacology, School of Medicine, College of Medicine, Taipei Medical University.*

[g] *Ph.D. Program in Biotechnology Research and Development, College of Pharmacy, Taipei Medical University.*

[h] *Traditional Herbal Medicine Research Center of Taipei Medical University Hospital, Taipei 11031, Taiwan.*

Abstract: This study reports the synthesis of a series of 1-aroylisoindoline hydroxamic acids employing N-benzyl, long alkyl chain and acrylamide units as diverse linkers. *In-vitro* studies led to the identification of N-benzyl linker-bearing compound (**10**) and long chain linker-containing compound (**17**) as dual selective HDAC6/HSP90 inhibitors. Compound **17** displays potent inhibition of HDAC6 isoform (IC_{50} = 4.3 nM) and HSP90a inhibition (IC_{50} = 46.8 nM) along with substantial cell growth inhibitory effects with GI_{50} = 0.76 µM (lung A549) and GI_{50} = 0.52 µM (lung EGFR resistant H1975). Compound **10** displays potent antiproliferative activity against lung A549 (GI_{50} = 0.37 µM) and lung H1975 cell lines (GI_{50} = 0.13 µM) mediated through selective HDAC6 inhibition (IC_{50} = 33.3 nM) and HSP90 inhibition (IC_{50} = 66 nM). In addition, compound **17** also modulated the expression of signatory biomarkers associated with HDAC6 and HSP90 inhibition. In the *in vivo* efficacy evaluation in human H1975 xenografts, **17** induced slightly remarkable suppression of tumor growth both in monotherapy as well as the combination therapy with afatinib (20 mg/kg). Moreover, compound **17** could effectively reduce programmed death-ligand 1 (PD-L1) expression in IFN-γ treated lung H1975 cells in a dose dependent manner suggesting that dual inhibition of HDAC6 and HSP90 can modulate immunosuppressive ability of tumor area.

Keywords: Isoindoline, programmed death-ligand 1 (PD-L1), Histone deacetylase, Heat shock protein, lung cancer

1. Introduction

Non-Small Cell Lung Cancer (NSCLC) accounts for more than 85-90 % of all lung cancers, a disease which is the leading cause of cancer-related mortality.[1-3] Arising from a complex series of genetic and epigenetic changes, NSCLC leads to uncontrolled cell growth and metastases and has a poor prognosis.[4-5] Several chemotherapy regimens have demonstrated efficacy, but the existing therapies have not been able to obtain satisfactory results in improving survival of NSCLC patients[3]. Often subclassified as molecularly defined oncogene addicted tumors, NSCLC suffers from the development of therapeutic resistance to targeted agents.[6,7] These factors clearly confirm the need for exploration of diverse mechanisms to accomplish therapeutic benefits in lung cancer along with a comprehensive understanding of the molecular heterogeneity in NSCLC that is necessary to design new anticancer agents.

The last decade has evidenced an exponential increase in the number of investigations on NSCLC by targeting of histone deacetylase (HDAC) enzymes and heat shock protein 90 (HSP90) chaperone proteins. HDAC inhibitors induce relief of transcriptional repression in various leukemias and are considered to be a key to epigenetic cancer therapy.[8,9] Several FDA approved HDAC inhibitors such as SAHA (**1**)[10], PXD101 (**2**)[11], LBH589 (**3**)[12] and Valproic acid (**4**)[13,14] have been extensively investigated in NSCLC at the clinical and the preclinical level. In addition to induction of apoptosis in NSCLC[15] or demonstration of synergistic antitumor efficacy in combination studies with established therapeutics[12, 16-19], HDAC inhibitors have also exhibited potential for sensitizing NSCLC to ionizing radiations.[20] These facts place this therapeutic class in the forefront of the investigations presently being conducted for NSCLC. Concomitantly HSP90 inhibition has also emerged as a logical strategy in drug design for NSCLC. HSP90 is a chaperone protein that protects other cellular proteins from degradation by the ubiquitin-proteasome system

in conditions of stress[21]. Preclinical HSP90 inhibitors are endowed with significant potential in NSCLC, either alone or in combination.[22] In particular, second generation HSP90 inhibitors such as IPI-504 (**5**)[23], BIIB021 (**6**)[24], AUY922 (**7**)[25], Ganetespib (**8**)[26] and AT13387 (**9**)[27] have shown promise in distinct molecular subtypes, such as ALK, KRAS, EGFR, and HER2 in early clinical trials. Despite the documented promise in preclinical studies and early phase clinical trials, HSP-90 inhibitors have not been able to replicate their effectiveness at higher stage clinical stages.[22, 28-30] Thus, fabrication of rationally designed strategies to extract the potential of HSP90 inhibition is required to ascertain conclusive benefits in NSCLC.

It has been well reported that HDAC inhibitors induce acetylation and inhibit the ATP binding and chaperone functions of HSP90 leading to the degradation of pro-survival client proteins in human leukemia cells.[31-33] Synergistic reports of pan HDAC and selective HDAC6 inhibitors with HSP90 inhibitors further rationalizes this biochemical relation[34]. Moreover, a recent investigation by Deskin *et al.* reported that targeting the HDAC6/HSP90 Axis to destabilize the notch1 receptor in NSCLC may offer therapeutic benefits in NSCLC as both HDAC6 and HSP90 regulate Notch1 receptor levels through the ubiquitin proteasome system.[35] In light of these optimistic revelations, development of dual HDAC-HSP90 inhibitors is anticipated to yield favorable outcomes in NSCLC therapy.

Our previous investigations on small molecule HDAC inhibitors revealed key structural insights critical for modulating the enzymatic activity and influencing the cellular activity. These identified structural features include a flexibility in the chemical nature of the CAP constructs that tolerates variability from bicyclic planar to non-planar/partially hydrogenated (6,6/6,5-fused) heteroaryl rings as well as the linkers and the critical point of attachment of the zinc binding motif to the heteroaryl rings. [36, 37] Capitalizing on this structural information, the present study broadens

the investigation parameters of our ongoing drug discovery program towards the design of HDAC inhibitors capable of modulating the HSP90 chaperone. The design strategy involved the utilization of amide tethered resorcinol-isoindoline functionality as an extended CAP component of the HDAC inhibitory scaffold. The resorcinol fragment has been recognized as a crucial structural unit present in several second generation HSP90 inhibitors [23, 25, 26, 27] and serves as a key binder associated with the ATP binding site of HSP90 proteins by means of an appropriate fit in the hydrophilic and hydrophobic regions of the protein[38]. Specifically, the selection of isoindoline - resorcinol adduct as the surface recognition part was influenced due to the following reasons : a) recent optimistic reports of N-heterocyclic ring linked resorcinol adducts as HSP90 inhibitors [39] b) existence of the structural unit composed of isoindoline core condensed with resorcinol ring in the chemical architecture of AT-13387, a second generation HSP90 inhibitor undergoing clinical studies in NSCLC[27] c) recent study by our research group demonstrating the potential of indoline based hydroxamic acids as dual HDAC/HSP90 inhibitors [36]. Moreover, several alterations were attempted in the chemical architecture of designed hybrids in the context of the linker type (long chain alkyl, benzyl and acrylamide functionality), however the positioning of zinc binding motif on the non-planar isoindoline ring using diverse linkers was kept constant. With this background, we report herein the synthesis and biological evaluation of a series of 1-aroylisoindoline-hydroxamic acids as dual inhibitors of HDAC and HSP90. In addition to enzymatic and cellular activity (*in-vitro* and *in-vivo*), the potential of the synthetic compounds to upregulate/downregulate the expressions of signatory biomarkers associated with HDAC and HSP 90 inhibition was investigated. A docking study was also performed to examine the key interactions of the designed synthetic compounds, the selected compounds, with the amino acid residues and support the basis of inhibition of HDAC6 isoform along with the HSP90 chaperone.

The effect of one of the potent hydroxamic acid was also studied on the IFN-γ induced PDL-1 expression in H1975 lung cancer cells to evaluate the potential of dual HDAC/HSP90 inhibition towards the modulation of immunosuppressive ability of tumor area.

2. Results

2.1 Chemistry

Synthetic routes for the designed compounds are depicted in Schemes 1, 2 and 3. Scheme 1 illustrates the synthesis of the N-benzyl linker-based target compound and the methodology starts with the nitration of isoindoline (**19**) which yields nitroisoindoline (**20**, yield 50 %) with a moderate yield. This nitrated isoindoline was subjected to EDC/HOBT assisted amidation with 2,4-bis(benzyloxy)-5-isopropylbenzoic acid to generate the amide (**21**, yield 70 %) which underwent Fe/NH_4Cl mediated nitro reduction to produce the primary amine (**22**, yield 80 %) which on reductive amination yielded the secondary amine (**23**, yield 75 %). Lithium hydroxide assisted ester hydrolysis of **23** produced the carboxylic acid (**24**, yield 96 %) which upon amidation with NH_2OBn followed by BCl_3-catalyzed debenzylation furnished the target hydroxamic acid (**10**, yield 97 %).

To establish the influence of various linkers on the bioactivity, long chain linker based hydroxamic acids (**11**-**17**) were synthesized using the strategy shown in Scheme 2. The implementation of the similar methodology i.e EDC/HOBT mediated amide bond formation with alkoxyalkanoic acids (**25**-**31**, yields 73-86 %), ester hydrolysis (**32**-**38**, yields 91-97 %) and amidation with NH_2OBn afforded the intermediates **39-45** (yields 71-82 %) which were debenzylated using 10% Pd/C in MeOH in a hydrogenation vessel with H_2 at 40 - 42 psi to afford the desired hydroxamic acids (**11-17**, yields 70-78 %)**.** Attempts to further ascertain the linker-

activity correlation led us synthesize a short linker, an acrylamide bearing a hydroxamic acid **(18)**. The synthetic route to the target compound (**18**) begins with the $NaBH_4$ reduction of 5-bromoisoindoline-1,3-dione (**46**) to 5-bromoisoindoline (**47**, yield 59 %). Amidation of **47** with 2,4-bis(benzyloxy)-5-isopropylbenzoic acid (**48**, yield 75 %) followed by $Pd(OAc)_2$-catalyzed Heck olefination with methyl acrylate yielded the intermediate **49** (yield 53 %). The Heck coupled product (**49**) underwent lithium hydroxide assisted ester hydrolysis, amidation with NH_2OBn and BCl_3 catalyzed debenzylation to produce the target hydroxamic acid (**18**, yield 66 %).

2.2 Biological evaluation

2.2.1 *In vitro* cytotoxicity studies

The synthesized compounds were assayed for growth inhibition of non-small cell lung cancer A549 and H1975 cells. The GI_{50} values, defined as concentrations of the compounds that induced 50% cell growth inhibition were determined and the summarized results are shown in Table 1. SAHA (**1**), an FDA approved HDAC inhibitor and BIIB021 (**6**), an orally available small-molecule HSP90 inhibitor were employed as standards in the study. The synthetic compounds were designed to ascertain the impact of diverse linkers, i.e the N-benzyl, long alkyl chain and acrylamide linker on the cellular activity. Among the tested compounds, compound **10** bearing the N-benzyl linker exhibited the most substantial cytotoxic effects against A549 cell lines and H1975 cell line with GI_{50} values of 0.37 µM and 0.13 µM, respectively. It was interesting to observe that the cell growth inhibitory effects of **10** against A549 and H1975 cell lines were more pronounced than those of **1**, which was the standard employed. Specifically, the effects of **10** against non-small cell lung cancer cell lines H1975 cell lines were higher than those of both the

standards employed (**1** and **6**). Use of the alkyl chain in place of the N-benzyl linker failed to yield favorable results in the context of potentiating the antiproliferative effects in a relative comparison. Among the alkyl chain linker bearing compounds, compound **11** (n = 2) exhibited significant cell growth inhibitory effects against both NSCLC cell lines with higher sensitivity towards H1975 cell lines (IC_{50} value = 0.39 µM). In general, a variable cytotoxic profile of alkyl chain linker based compounds (**11-17**) was observed towards the cell lines tested. It was observed that extending the linker length to n = 3 led to dramatic loss of activity as evidenced by compound **12**. Potency was found to be regenerated by extending the methylene chain length as in compound **13** (n = 4) but an exact dependence of linker length and a compound's ability to exhibit cellular activity was found to be variable for compounds **13-17,** (n = 4-8). Compound **17** (n = 8) displayed a balanced cytotoxic profile against both the NSCLC cell lines with GI_{50} = 0.76 µM in A549 cells and GI_{50} = 0.52 µM in H1975 cells. Further introduction of an acrylamide linker at position 5 of the isoindoline ring (**18**) led to selective antiproliferative effects about 9-fold better against H1975 cell line (GI_{50} = 0.32 µM) than against the A549 cell line (GI_{50} = 2.74 µM), however it turned out to be less effective than its counterpart (compound **10**) bearing the N-benzyl linker. In general, all the compounds except compounds **13** and **15** displayed a similar trend of higher effectiveness towards H1975 cell lines. Overall, compounds **10**, **11** and **17** have significant inhibitory potential against both the NSCLC cell lines employed.

2.2.2 HeLa nuclear HDAC enzyme inhibition and Heat Shock protein 90 inhibition

Evaluation of HDAC inhibitory activity using HeLa nuclear extract as the HDAC source was conducted (Table 2). The correlation of the HDAC inhibitory activity of the synthetic compounds with the linker length led to interesting results and demonstrated that the length of the linker for

compound **11 - 17** was instrumental in modulating the HDAC inhibition. It was observed that compounds **11 - 13** (n = 2-4) were devoid of HDAC inhibition and extension of linker length beyond n = 4 induced the inhibitory potential towards the HeLa HDAC. The long chain linker **15**, bearing a hydroxamic acid (n = 6) and possessing the same combination of the linker and the zinc binding motif as that of compound **1** displayed the most potent inhibitory activity with IC_{50} = 168.3 nM. Among the three most cytotoxic compounds **10, 11, 17**, only **17** (n = 8, IC_{50} = 388.8 nM) exhibited HeLa nuclear HDAC inhibitory potential. The hydroxamic acids **10** (with benzyl linker) and **11** (n = 2) displayed diminished activity against the HeLa HDAC. Contrary to the results of HeLa HDAC inhibition, an HSP90 inhibitory assay, employing compound **6** as a standard indicated that all the compounds are potent HSP90 inhibitors with IC_{50} values ranging from 42.2 - 135.6 nM (Table 2). In particular, the pronounced effects of compounds **14-17** (n = 5-8, IC_{50} = 42.2 – 46.8 nM) against the chaperone protein are higher than those of the standard (**6**). Compounds **15** [(IC_{50} = 43.9 nM (HSP90), 168.3 nM (HDAC)] and **16** [(IC_{50} = 42.2 nM (HSP90), 198.9 nM (HDAC)] were found to be the most potent dual inhibitors of HeLa HDAC and HSP90. Overall, the ability of the compounds to inhibit HSP90 protein was influenced only marginally by the linker length and could be attributed to the presence of isopropyl resorcinol fragment in the chemical architecture of the synthesized compounds. All the three potent antiproliferatives **10**, **11** and **17** modulated the activity of HSP90 with IC_{50} values of 66, 123.1 and 46.8 nM, respectively. Compound **18** failed to alter the activity of the HeLa HDAC enzyme and only modulated the HSP90 activity.

2.2.3 HDAC isoform inhibition

Isoform selective inhibitory effects were examined for the synthesized adducts towards the HDAC 1, 3, 6 and 8 isoform employing trichostatin A as the reference compound. The results summarized in Table 3 indicate that HDAC6 isoform was the most sensitive to the exposure of all the compounds. The impact of the linker variation on HDAC6 inhibition was clearly observed with the N-benzyl group and a long chain linker (n = 5-8) demonstrating favorable trends towards the inhibition of HDAC6 isoform. Compound **10** bearing the N-benzyl linker was effective in inhibiting the HDAC6 isoform (IC_{50} = 33.3 nM) with a selectivity of 300 and 296 fold over HDAC1 and **3**. In addition, adduct **10** also moderately inhibited the HDAC8 isoform. Concomitant evaluation of the HDAC isoform inhibitory ability of the long chain linker bearing hydroxamic acids (**11-17**) revealed an interesting linker-HDAC6 inhibition relationship. The correlation of results presented in Table 1, 2 and 3 showed that compound **11** (n = 2) induces cell growth inhibitory effects against the NSCLC solely through HSP90 inhibition and is devoid of inhibitory effects against the HDAC isoforms. A dramatic amplification in the HDAC6 inhibitory activity was observed on extension of the methylene chain from **11** (n = 2, IC_{50} >10,000 nM), to **12** (n = 3, IC_{50} = 68.6 nM), but a further increase in the chain length (n = 4, IC_{50} = 330 nM) did not replicate the similar positive trends towards HDAC 6 inhibition. A continuing variable pattern was seen in the influence of chain length on enzymatic activity and lengthening the methylene chain from n = 4 to n = 5-8 led to marked increase in the activity profile of hydroxamic acids (**14-17**) against the HDAC6 isoform. The hydroxamic acids (**14-17**) were endowed with IC_{50} values in single digit nanomolar range (HDAC6 inhibition). Overall, a linker length of n = 6 - 7 was the most suitable for inducing HDAC 6 inhibition and compounds **15** (n = 6, IC_{50} = 2.21 nM**)** and **16** (n = 7, IC_{50} = 2.12 nM) were identified as the most potent HDAC6 inhibitors exhibiting higher HDAC6 inhibitory effects than even the standard trichostatin A (**1**, IC_{50} = 2.60 nM). Compound

15 displayed 250, 175 and 683 fold higher selectivity for HDAC 6 than the HDAC1, 3 and 8 isoforms. Similarly, inhibitor **16** also exerted preferential effects against the HDAC6 isoform with a selectivity ratio of 507 for HDAC1/HDAC6, 233 for HDAC3/HDAC6 and >4716 for HDAC8/HDAC6. Among the three most potent cytotoxic compounds **10**, **11** and **17**, the HDAC6 isoform was most significantly inhibited by **17** with an IC_{50} value of 4.32 nM. Compound **17** was also highly selective against HDAC6 in comparison to HDAC1, HDAC3 and HDAC8 by factors of 434, 303 and 861 respectively. The insertion of the -C=C- linkage between N-hydroxyaminocarbonyl and isoindoline ring (**18**) led to significant loss of the enzymatic potency (HDAC6) and the acrylamide linker containing hydroxamic acid (**18**) displayed only moderate inhibition of the HDAC6. In summary, this study confirms the influence of diverse linkers on the selective HDAC 6 inhibition.

2.2.4 Western Blot Analysis

In view of the balanced modulation of HeLa HDAC, HDAC6 isoform and HSP90 along with the potent antiproliferative effects against NSCLC, the ability of compound **17** to downregulate/upregulate the protein levels of important biomarkers associated with intracellular HDAC inhibition was determined. For the western blot analysis, H1975 cells were treated with **17** or SAHA at the indicated concentrations for 24 h (Figure 2). The results demonstrate that compound **17** induced upregulation of acetylated α-tubulin in a dose-dependent manner and this feature is consistent with the signatory feature of HDAC6 inhibitors. Western blot analysis was also conducted to evaluate the degradation of multiple HSP90 client proteins triggered by compound **17** in concentration and time-dependent manners. Figure 3A presents the results obtained when H1975 cells were treated with DMSO or 0.03-3 μM of test compounds (**17**,

BIIB021, and Tubastatin A) for 24 h and Figure 3B presents the results for the treatment of H1975 cells were treated with 3 μM of **17** for indicated times. Acetylated-tubulin was induced much greater by **17** compared to Tubastatin A at the same concentrations (Figure 3A). A notable induction of chaperone protein HSP70 and downregulation of the well-known HSP90 client protein Akt were observed in cells (Figure 3A). These results represents the characteristic molecular signature of HSP90 inhibition. In addition, activated Akt (p-Akt Ser473) was reduced at early 6 h treatment time point followed by downregulation of activated Stat3 (p-Stat3 Tyr705) at 12 h time point. We further compared **17** with another reference compound AT-13387 which is also consisting of resorcinol tethered isoindoline ring to inhibit HSP90 activity. As shown in Figure 3C, both of **17** and AT-13387 exhibit potent inhibitory activity on survival signals (activated Akt and Stat3). Although it has been reported AT-13387 downregulates HDAC6 expression to stabilize the acetylated α-tubulin[40], our result shows **17** is a more potent inducer of acetylated tubulin than AT-13387 at the same concentrations, suggesting **17** may have more impacts of microtubule-associated proteins to regulate cell migration compared to AT-13387. Taken together, the results confirm that the cell killing effects of **17** stems from modulation of HSP90 protein in addition to HDAC inhibition.

Moreover, compound **17** activates cell accumulation at the subG1 phase as shown by propidium iodide staining and flow cytometry analysis (Fig. 4A), suggesting compound **17** displays potent cytotoxicity against H1975 cancer cells. We further observed that compound **17** induces concentration-dependent activation of caspase 3/8/9, PARP, and γH2AX (Fig. 4B), indicating that compound **17** is a potent inducer of apoptosis in H1975 lung cancer cells.

2.2.5 Molecular modeling study

A molecular docking study was performed for compounds **10** and **17** to identify the important interactions with the amino acid residues of HSP90 and HDAC6. The docking protocol used in this study was first validated by redocking the co-crystallized ligands of HSP90, HDAC1 and HDAC6 (Fig. 5). The co-crystalized ligand of the HDAC3 structure was not included for validation because it is an acetate molecule that was used for the refinement process of crystallization[41]. The redocked ligands produced poses similar to those of the co-crystallized ligands for HSP90, HDAC1 and HDAC6, indicating that a rational docking protocol was used.

It was observed that when compound **17** binds to HSP90, it adopts a U-shape (Fig. 6). The compound structure can be divided into four groups. Group 1 is composed of 2,4-dihydroxy-5-isopropylbenzoyl functionality. This group forms hydrogen bonds with residues N51, D93 and T184 in HSP90 and is also involved in hydrophobic interactions with residues F138 and T184. Group 2 consists of an N-(2,3-dihydro-1H-isoindol-5-yl)formamide moiety and forms hydrogen bonds with residues K58 and G108. Both Group 2 and Group 3, which consists of an eight carbon-chain occupy a hydrophobic pocket and interact with residues A55 and M98. These interactions sandwich Group 2 and Group 3 along the outer rim of the HSP90 binding site (Fig. 6). Group 4 consists of a hydroxamic acid moiety and is involved in hydrogen bonding interactions with residues E47, N51 and G137 of the protein. This moiety binds to the entrance of the binding site and forms additional hydrogen bonds (Figs. 6A and 6B).

Compound **10** displays a similar docking pose and can also be separated into four groups. Group 1 consists of a 2,4-dihydroxy-5-isopropylbenzoyl moiety and creates hydrogen bonds with residues N51, D93 and T184. Group 2 and Group 3 contain a 2,3-dihydro-1H-isoindol-5-amine and a benzyl moiety, respectively (Fig. 6D). No hydrogen bonds were observed with these groups. This may account for the weaker activity of compound **10** towards HSP90 as compared to

compound **17**. Hydrophobic interactions with residues A55, M98 and T109 sandwich Group 2 and Group 3 along the outer rim of the binding site (Fig. 6C). Finally, Group 4 bearing a hydroxamic acid moiety forms hydrogen bonds with N51, G135 and F138. These hydrogen bonds differ from those observed with compound **17**. Compound **17** contains an eight-carbon chain at Group 3 which increases its overall length. As a result, compound **10** is unable to create hydrogen bonds with the same residues as compound **17**. Together, these interactions suggest that compound **17** and compound **10** anchor to the binding site and thus inhibit HSP90 function.

Compounds **17** and **10** were docked to HDAC6 and the interactions between the compounds and the catalytic site were analyzed. HDAC inhibitors typically contain three conserved structures: a cap that obstructs the binding site entrance, a linker that connects the two structures and a zinc binding group (ZBG).[42] Both compound **17** and compound **10** contain these structural hallmarks where Group 1 and Group 2 act as the cap construct, Group 3 forms the linker and Group 4 acts as a zinc binding group (Fig. 7A-B). The cap of compound **17** creates hydrogen bonds with residues S564, F566 and I569. The linker of compound **17** spans the hydrophobic channel of HDAC 6 and hydrophobic interactions are observed with residue F620. The ZBG of compound **17** extends into the HDAC6 catalytic site. Compound **17** contains a hydroxamate acid as the ZBG and coordinates to the zinc ion in a bidentate mode (Fig. 7C). Additional hydrogen bonds are formed with nearby residues. For example, residue H610 forms a hydrogen bond to the hydroxamate N-O group (distance 3.1Å) and residue G619 forms a hydrogen bond to the hydroxamate NH group (distance 3.0Å). These interactions suggest that compound **17** creates sufficient interactions within the HDAC6 catalytic site.

An analysis of compound **10** was performed and compared to compound **17**. Compound **10** contains the same cap structure (Fig. 7B). This facilitates similar hydrogen-bonding interactions

with residues S564, F566 and I569 at the periphery of the HDAC6 binding site. The linker of compound **10** spans the hydrophobic channel of the binding site (Fig. 7B). Compound **10** contains an aromatic ring-based linker, making it more rigid than compound **17**. Hydrophobic interactions occur between the linker and residues H651, F680 and L749. The ZBG of Compound **10** contains a hydroxamic moiety attached to a sterically bulky aromatic ring. It has been reported in the literature that compounds with sterically bulky substituents, such as ACY-1083, coordinates to the HDAC 6 Zn^{2+} in a monodentate fashion.[43,44] A water molecule was added to the binding site during the docking analysis. The docking result showed compound **10** coordinates to the Zn^{2+} in the monodentate mode, with one hydroxamate oxygen atom interacting with the Zn^{2+} atom and another oxygen atom hydrogen-bonding with a water molecule (distance 2.7Å) (Fig. 7D). An additional hydrogen bond is formed between the hydroxamate NH group and residue G619 (distance 2.7Å). Together, our analysis shows that compound **17** and compound **10** can bind to the HDAC 6 catalytic site and coordinate to the Zn^{2+} ion, which suggests that it makes favorable interactions for HDAC6 inhibition.

For HDAC6 inhibition, we found that compound **10** has lower activity when compared to compound **17**. A relative comparison of the docking results of compound **10** and **17** revealed different interactions along the periphery of the hydrophobic tunnel (Fig. 7E-F). Residue L749 is found along the hydrophobic channel periphery. Compound **17** contains an eight-carbon chain linker that forms a hydrophobic interaction with residue L749 (Fig. 7E). In contrast, the linker of compound **10** contains an aromatic ring and is a relatively more rigid structure. Our docking result showed that the compound **10** linker does not form interactions with residue L749 (Fig. 7F). Together, the different interactions between the linker and the hydrophobic tunnel may account for reduced activity of compound **10**.

To further identify the reasons HDAC6 selectivity towards, we docked compound **17** into HDAC1 and HDAC3. Superimposing the HDAC1, 3 and 6 binding site revealed a specific pocket observed in HDAC6 (Fig. 8A). The compound **17** cap forms hydrogen bonds with residues S564, F566 and I569 (Fig. 8B). In addition, the hydrophobic channel consists of residues that create a larger cavity at the outer rim for the compound **17** cap. HDAC1 and HDAC3, in contrast, do not have a corresponding pocket on the surface and contain a loop which interferes with the cap interactions (Fig. 8B). As a result, compound **17** show greater specificity towards HDAC6.

To summarize, the docking study indicates that compound **17** and compound **10** target both the HSP90 chaperone and the HDAC6 isoform. The two active compounds share structures and interactions that can be separated into four groups. Group 1 enters the HSP90 binding pocket. The co-crystallized HSP90 ligand, 2D9, contains a similar sub-structure to Group 1 of compound **17** and compound **10** that is buried deep into the HSP90 binding site.[45] However, in HDAC6, Group 1 is located in the periphery and forms part of the cap seen in traditional HDAC inhibitors. In contrast, Group 4 bearing the vital zinc binding group for HDAC6 inhibition is located near the outer margin of the HSP90 binding site. Group 2 and Group 3 link the terminal ends of both compounds in HSP90. Hydrophobic interactions were observed sandwiching these structures in compound **17** and **10**. In addition, the Group 2 of compound **17** forms hydrogen bonds with residues K58 and G108. Group 2 of both active compounds form part of the cap in HDAC6 and group 3 forms the linker, which spans the HDAC6 hydrophobic tunnel.

The variation in the activity profile of compound **10** and **17** can be attributed to the nature of the linker. Residue L749 along the outer rim of the HDAC6 hydrophobic channel (Fig. 8). This residue has the potential to obstruct the entrance of the zinc binding site. Compound **17** is more flexible and does not clash with residue L749. However, compound **10** contains an aromatic ring

that occupies a space close to residue L749. The aromatic ring also forms hydrophobic interactions with the periphery residues. Thus, the variation in the linker may account for the reduced activity seen with compound **10**. The results of the docking study revealed key interactions that could be responsible for dual inhibition of HSP90 and HDAC6.

Our assays found compound **17** and compound **10** to have greater selectivity towards HDAC6. A molecular docking analysis was performed to further study HDAC selectivity. While the ZBG plays a crucial role in inhibiting HDACs, it is thought that the HDAC inhibitor cap determines the selectivity.[42, 46] We found that the cap region of compound **17** targets residues S564, F566 and I569 (Fig. 8). This area constitutes a binding pocket absent from HDAC1 or HDAC3. The binding pockets for the cap in HDAC1 and HDAC3 do not present optimal binding of the two compounds created for this study.

2.2.6 Growth Inhibition of human EGFR-resistance NSCLC H1975 xenograft model *in vivo*.

For the *in vivo* studies, Fig. 9 shows the *in vivo* activity of compound **17** in human NSCLC H1975 xenograft model employing Afatinib as a reference compound. The results have indicated that administration of **17** (50 mg/kg, ip, qd) reduced the tumor volume (TGI = 44.8%, $*p < 0.05$). However, the inhibitory effect of **17** at 50 mg/kg were less significant than afatinib (20 mg/kg, $***p<0.001$). The *in-vivo* potential of compound **17** was also investigated at the concentration of 100 mg/kg which led to slightly higher suppression of tumor growth (TGI = 69.7%) than afatinib (TGI = 63.8%, 20 mg/Kg). The combination treatment of Afatinib with compound **17** (50 mg/kg, ip, qd, Afatinib – 20 mg/kg, $***p<0.001$) was also evaluated which led to marginally higher tumor growth inhibition than produced by Afatinib alone. The most substantial *in-vivo* efficacy (combination studies) was exhibited by the combination of compound **17** and Afatinib (compound

17 - 50 mg/kg, ip, qd, Afatinib - 20 mg/kg, ***p<0.001) and showed enhancement of tumor suppression by a 72.3% tumor growth inhibition (TGI). In addition, no significant differences in weight loss were observed during all the treatments.

2.2.7 Downregulation of IFN-γ induced PD-L1 expression in H1975 lung cancer cells

T cells, especially cytotoxic T cells, can infiltrate into the tumor area to eliminate tumor cells by releasing cytotoxins (perforins and granzymes) and inflammatory cytokines (IFN-γ and TNF-α). However, IFN-γ also triggers the expression of programmed death-ligand 1 (PD-L1) on the surface of many tumor cells, leading T-cell suppression and immune evasion of tumor cells from cellular cytotoxicity [47,48]. To investigate whether compound **17** affects the INFγ-induced PD-L1 expression, H1975 human non-small cell lung cancer cells were cotreated with variant concentrations of compound **17** and 20 ng/ml of IFN-γ. The Western blot analysis (Figure 10 A) shows that compound **17** effectively reduced PD-L1 expression in IFN-γ treated H1975 cells in a dose-dependent manner. To further elucidate the inhibited level of surface PD-L1 expression, treated H1975 cells were analyzed with flow cytometry (Fig. 10 B and C). The PD-L1 expression on cell surface induced by IFN-γ was significantly decreased after the treatment with the compound **17** at concentration above 0.3 μM. These results indicate that the compound **17** reversed the IFN-γ-mediated upregulation of PD-L1, suggesting a possible function of the compound **17** in destroying the immunosuppressive environment of tumor area. Since the hostile tumor microenvironment of solid tumors remains a challenge to T cell therapy, a combination of compound **17** and T cell immunotherapy might be worth investigating to develop an approach generating synergistic antitumor effects of chemotherapy and immunotherapy.

3. Conclusion

In this study, a series of 1-aroylisoindoline-hydroxamic acids has been synthesized. The impact of diverse linkers connecting the 1-aroylisoindoline moiety to the zinc binding motif on the bioactivity was studied. *In-vitro* cytotoxicity studies revealed that the N-benzyl linker-based inhibitor (**10**) was the most effective in suppressing cell growth in both the NSCLC cell lines employed. Incorporation of the alkyl chain and acrylamide linker in the chemical architecture of the designed synthetics failed to enhance the cytotoxic potential as seen in the relative comparison with compound **10**. Compounds **11** and **17** displayed the most substantial cell growth inhibitory effects among the hydroxamic acids bearing an alkyl chain linker. It was interesting to observe that compound **11** exercised its cytotoxicity solely through HSP90 inhibition as evidenced by enzymatic assays, whereas the inhibitor **17** was found to have a balanced antiproliferative and enzyme inhibitory profile towards both the targets. In general, all the compounds exhibit selective inhibitory activity against HDAC 6 isoform with few exceptions. an important finding of this study is that the most pronounced dual HDAC6/HSP90 inhibition induced by a compound bearing a long chain linker was by **15** (n = 6) which possesses the same combination of linker and zinc binding group as that of SAHA, however the cell growth inhibitory effects of **15** were not significant. The main finding of this study is the identification of compound **10** and **17** as dual selective inhibitors of the HDAC6 isoform as well as the HSP90 protein, inducing significant antiproliferative effects against the NSCLC cell lines employed with higher efficacy against H1975 cell lines. Compound **17** also induced upregulation of important biomarkers associated with intracellular HDAC inhibition along with the concomitant induction of chaperone protein HSP70 and degradation of HSP90 client proteins which are considered to be a molecular signature of HSP90 inhibitors. Molecular modeling studies were employed to rationalize and

support the experimental results and the key interactions of compound **10** and **17** with HSP90 chaperone along with the HDAC6 isoform were rationalized**.** The docking study suggested several notions for the differences in the activity profile of compounds **10** and **17** along with the selectivity of these compounds towards the HDAC6 isoform. The *in vivo* efficacy of compound **17** was also evaluated in human EGFR-resistance NSCLC H1975 xenograft model and it was found that this inhibitor, both alone and in combination with Afatinib induced significant tumor growth inhibition. Moreover, compound **17** could effectively reduce (PD-L1) expression in IFN-γ treated lung H1975 cells in a dose dependent manner suggesting that dual inhibition of HDAC6 and HSP90 can modulate immunosuppressive ability of tumor area. This also indicates that compound **17** in combination with T cell immunotherapy might be worth investigating to develop an approach generating synergistic antitumor effects of chemotherapy and immunotherapy. Overall, the cumulative results indicates that hydroxamic acids such as **17** could emerge as potential leads for further investigation to develop selective HDAC6/HSP90 inhibitors as potent anticancer agents for lung cancer and immunosuppression inhibitory activity. Thus this study concludes and ascertains that the selective HDAC6/HSP90 inhibition appears to be a potentially effective strategy to target NSCLC.

4. Experimental

4.1 Chemistry

Nuclear magnetic resonance spectra were obtained with a Bruker DRX-500 spectrometer operating at 300 MHz, with chemical shifts reported in parts per million (ppm, d) downfield from TMS as an internal standard. High-resolution mass spectra (HRMS) were measured with a JEOL (JMS-700) electron impact (EI) mass spectrometer. The purity of the final compounds was

determined to be ≥ 95%, using an Agilent 1100 series HPLC system using C-18 column (Agilent ZORBAX Eclipse XDB-C18 5 μm, 4.6 mm × 150 mm). Flash column chromatography was done using silica gel (Merck Kieselgel 60, No. 9385, 230-400 mesh ASTM). All reactions were carried out under an atmosphere of dry nitrogen

5-Nitroisoindoline (20)

Conc. H_2SO_4 (8 mL) was added dropwise at 0° C to a solution of isoindoline (**19**) (2 g) in DCM (10 mL), and the reaction mixture was stirred at rt for 10 min. DCM was evaporated under vacuum from the reaction mixture and conc. HNO_3 (2 mL) was added dropwise at 0 °C. The reaction mixture was stirred for 2 h at rt. Ice water was added to the reaction mixture then the reaction mixture was basified with sodium bicarbonate. Extraction was done with EtOAc (100 mL x 3) and the combined organic layer was dried over anhydrous $MgSO_4$ and concentrated under reduced pressure to give **20** in 50% yield; ^{1}H NMR (300 MHz, $CDCl_3$): δ 8.07 - 8.12 (m, 2 H), 7.34 (d, *J* = 8.5 Hz, 1H), 4.32 (s, 4H).

(2,4-Bis(benzyloxy)-5-isopropylphenyl) (5-nitroisoindolin-2-yl) methanone (21)

A mixture of 3,5-bis(benzyloxy)-2-isopropylbenzoic acid (2.29 g, 6.09 mmol), EDC.HCl (1.88g, 12.18 mmol), HOBt (1.39 g, 9.13 mmol) and DIPEA (1.96 g, 15.22 mmol) in DCM (10 mL) was stirred at rt for 30 min before adding 5-nitroisoindoline (**20**) (1 g, 6.09 mmol). After being stirred for a further 5 h, the reaction mixture was quenched with H_2O and extracted with EtOAc (50 mL x 3). The combined organic layer was dried over anhydrous $MgSO_4$ and concentrated under reduced pressure. The residue was purified by silica gel chromatography (EtOAc:n-hexane = 1:4) to give **21** in 70% yield. ^{1}H NMR (300 MHz, $CDCl_3$): δ 8.19-8.20 (m, 2H), 7.98 (s, 1H), 7.10 -

7.45 (m, 11 H), 6.59 (s, 1H), 5.05 (s, 4H), 4.87 (s, 2H), 4.42 (s, 2H), 3.34 (m, 1H), 1.22 (d, *J* = 6.9 Hz, 6H).

(2,4-Bis(benzyloxy)-5-isopropylphenyl) (5-aminoisoindolin-2-yl) methanone (22)

A mixture of compound **21** (1.5 g, 2.8 mmol), Fe powder (801 mg, 14.3 mmol) and NH_4Cl (304 mg, 5.7 mmol) in EtOH (40 mL) and H_2O (10 mL) was refluxed for 2 h. The progress of the reaction was monitored by TLC. After completion of the reaction, the reaction mixture was filtered over celite. To the filtrate, H_2O (50 mL) was added and extraction was done with EtOAc (50 mL x 3). The combined organic layer was dried over anhydrous $MgSO_4$ and concentrated under reduced pressure. The residue was purified by silica gel chromatography (EtOAc:n-hexane = 2:3) to give **22** in 80% yield. ^{1}H NMR (300 MHz, CD_3OD): δ 7.10 -7.45 (m, 14 H), 6.56 (s, 1H), 5.16 (s, 2H), 5.12 (s, 2H), 4.75 (s, 2H), 4.39 (s, 2H), 3.32 (1H, m), 1.23 (d, *J* = 6.9 Hz, 6H).

4-{[2-(2,4-Bis-benzyloxy-5-isopropyl-benzoyl)-2,3-dihydro-1H-isoindol-5-ylamino]-methyl}-benzoic acid methyl ester (23)

Methyl 4-formylbenzoate (366 mg, 2.23 mmol) and a few drops of glacial AcOH were added to the solution of compound **22** (1 g, 2.03 mmol) in EtOH. The reaction mixture was stirred at rt for 30 min then $NaBH_3CN$ (191 mg, 3.04 mmol) was added to the reaction mixture and stirring was continued for 4 h at rt. The reaction mixture was quenched with H_2O and extracted with EtOAc (100 mL x 3). The combined organic layer was dried over anhydrous $MgSO_4$ and concentrated under reduced pressure. The residue was purified by silica gel chromatography (EtOAc:n-hexane = 3:2) to give **23** in 75% yield. ^{1}H NMR (300 MHz, CD_3OD): δ 7.99 (d, *J* =8.1 Hz, 2H), 7.13 - 7.47 (m, 16 H), 6.80 (s, 1H), 5.05 (s, 2H), 5.03 (s, 2H), 4.87 (s, 2H), 4.42 (s, 2H), 4.40 (s, 2H), 3.91 (s, 3H), 3.35 (1H, m), 1.20 (d, *J* = 6.9 Hz, 6H).

4-{[2-(2,4-Bis-benzyloxy-5-isopropyl-benzoyl)-2,3-dihydro-1H-isoindol-5-ylamino]-methyl}-benzoic acid (24)

A mixture of compound **23** (800 mg, 1.2 mmol), 1 M LiOH (aq) (6 mL) and dioxane (10 mL) was stirred at 40 °C for 2 h. The reaction was concentrated under reduced pressure and H_2O was added. The mixture was acidified with 3 N HCl and extracted with EtOAc (50 mL x 3). The combined organic layer was dried over anhydrous $MgSO_4$ and concentrated under reduced pressure to yield the acid (**24**) in 96% yield; ^{1}H NMR (300 MHz, CD_3OD): δ 8.02 (d, *J* =8.1 Hz, 2H), 7.17 -7.49 (m, 16 H), 6.82 (s, 1H), 5.16 (s, 2H), 5.12 (s, 2H), 4.75 (s, 2H), 4.40 (s, 2H), 4.39 (s, 2H), 3.39 (m, 1H), 1.22 (d, *J* = 6.9 Hz, 6H).

4-(((2-(2,4-Dihydroxy-5-isopropylbenzoyl) isoindolin-5-yl) amino) methyl)-N-hydroxy-benzamide (10)

A mixture of compound **24** (750 mg, 1.19 mmol), EDC.HCl (494 mg, 2.39 mmol), HOBt (242 mg, 1.79 mmol) and DIPEA (385 mg, 2.99 mmol) in DMF (5 mL) was stirred at rt for 30 min before adding NH_2OBn.HCl After being stirred for a further 5 h, the reaction mixture was quenched with H_2O and extracted with EtOAc (100 mL x 3). The combined organic layer was dried over anhydrous $MgSO_4$ and concentrated under reduced pressure. The residue was purified by silica gel chromatography (EtOAc) to give a semisolid product. The resulting product was dissolved in DCM (100 mL). BCl_3 (1 M in heptane, 6 eq) was added to this solution at 0 °C and the reaction mixture was stirred for 45 min at the same temperature. The progress of the reaction was monitored by TLC. The reaction mixture was filtered to collect the precipitated solid (**10**, 97% yield). HPLC purity: 97.19%. mp: 100-101 °C; ^{1}H NMR (300 MHz, CD_3OD): δ 7.81 (d, *J* = 8.1 Hz, 2H), 7.57 (d, *J* = 8.1 Hz, 2H), 7.46-7.47 (m, 2H), 7.36 (d, *J* = 8.1 Hz, 1 H), 7.18 (s, 1H), 6.43 (s, 1H), 5.04 (s, 4H), 4.70 (s, 2H), 3.22 (m, 1H), 1.23 (d, *J* = 6.9 Hz, 6H); ^{13}C NMR (75 Hz,

CD_3OD): δ 168.40, 163.21, 155.390, 151.36, 131.77, 131.42, 130.47, 127.96, 125.64, 125.53, 124.77, 124.27, 122.95, 121.69, 119.95, 115.11, 109.74, 99.72, 52.28, 23.69, 19.09; HRMS (ESI) for $C_{26}H_{26}N_3O_5$ $(M-H)^-$: calcd, 460.1872; found, 460.1867.

Methyl 4-((2-(2,4-bis(benzyloxy)-5-isopropylbenzoyl) isoindolin-5-yl) amino)-4-oxobutanoate (25)

A mixture of **22** (0.3 g, 0.609 mmol), EDC.HCl (0.232 g, 1.21 mmol), HOBt (0.123 g, 737 mg, 0.914 mmol), 4-methoxy-4-oxobutanoic acid (0.96 g, 0.727 mmol) and DIPEA (0.265 mL, 1.52 mmol) in DMF (5 mL) was stirred at rt for 5 h. After being stirred for a further 5 h, the reaction mixture was quenched with H_2O and extracted with EtOAc (50 mL x 3). The combined organic layer was dried over anhydrous $MgSO_4$, concentrated under reduced pressure and purified by silica gel chromatography (hexane : EtOAc = 4 : 1) to give **25** in 80% yield; ^{1}H NMR (300 MHz, $CDCl_3$): δ 7.13 -7.54 (m, 14H), 6.48 (s, 1H), 5.14 (s, 4H), 4.74 (bs, 4H), 3.64 (s, 3H), 3.14 (m, 1H), 2.21 (t, *J* = 6.9 Hz, 2H), 2.15 (t, *J* = 7.5 Hz, 2H), 1.12 (d, *J* = 6.9 Hz, 6H).

Methyl 5-((2-(2,4-bis(benzyloxy)-5-isopropylbenzoyl) isoindolin-5-yl) amino)-5-oxopent-anoate (26)

The title compound **26** was obtained in 82% yield from compound **22** using 5-methoxy-5-oxopentanoic acid in a manner similar to that described for the synthesis of compound **25;** ^{1}H NMR (300 MHz, $CDCl_3$): δ 7.11 -7.51 (m, 14H), 6.42 (s, 1H), 5.11 (s, 4H), 4.78 (bs, 4H), 3.59 (s, 3H), 3.12 (m, 1H), 2.29 (t, *J* = 6.9 Hz, 2H), 2.07 (bs, 2H), 1.98 (m, 2H), 1.15 (d, *J* = 6.9 Hz, 6H).

Methyl 6-((2-(2,4-bis(benzyloxy)-5-isopropylbenzoyl) isoindolin-5-yl) amino)-6-oxo hexan-ate (27)

The title compound **27** was obtained in 86% yield from compound **22** using 6-methoxy-6-oxohexanoic acid in a manner similar to that described for the synthesis of compound **25**; ^{1}H NMR (300 MHz, $CDCl_3$): δ 7.09 -7.54 (m, 14H), 6.47 (s, 1H), 5.11 (s, 4H), 4.85 (bs, 4H), 3.62 (s,

3H), 3.09 (m, 1H), 2.21 (t, *J* = 6.9 Hz, 2H), 2.11 (bs, 2H), 1.69-1.75 (m, 4H), 1.18 (d, *J* = 6.9 Hz, 6H).

Methyl 7-((2-(2,4-bis(benzyloxy)-5-isopropylbenzoyl) isoindolin-5-yl) amino)-7-oxoheptanoate (28)

The title compound **28** was obtained in 79% yield from compound 2**2** using 7-methoxy-7-oxoheptanoic acid in a manner similar to that described for the synthesis of compound **25**; ^{1}H NMR (300 MHz, $CDCl_3$): δ 7.12 -7.48 (m, 14H), 6.42 (s, 1H), 5.11 (s, 4H), 4.81 (bs, 4H), 3.61 (s, 3H), 3.11 (m, 1H), 2.13 (t, *J* = 6.9 Hz, 2H), 2.08 (bs, 2H), 1.64-1.78 (m, 4H), 1.45 (bs, 2H), 1.21 (d, *J* = 6.9 Hz, 6H).

Methyl 8-((2-(2,4-bis(benzyloxy)-5-isopropylbenzoyl) isoindolin-5-yl) amino)-8-oxooctanoate (29)

The title compound **29** was obtained in 76% yield from compound **22** using 8-methoxy-8-oxooctanoic acid in a manner similar to that described for the synthesis of compound **25**; ^{1}H NMR (300 MHz, $CDCl_3$): δ 7.11 -7.55 (m, 14H), 6.49 (s, 1H), 5. 08 (s, 4H), 4.88 (bs, 4H), 3.65 (s, 3H), 3.15 (m, 1H), 2.20 (bs, 2H), 2.11 (t, *J* = 6.3 Hz, 2H), 1.58-1.61 (m, 4H), 1.28 (bs, 4H), 1.18 (d, *J* = 6.6 Hz, 6H).

Methyl 9-((2-(2,4-bis(benzyloxy)-5-isopropylbenzoyl) isoindolin-5-yl) amino)-9-oxonon-anoate (30)

The title compound **30** was obtained in 86% yield from compound **22** using 9-methoxy-9-oxononanoic acid in a manner similar to that described for the synthesis of compound **25**; ^{1}H NMR (300 MHz, $CDCl_3$): δ 7.13 -7.51 (m, 14H), 6.43 (s, 1H), 5.12 (s, 4H), 4.82 (bs, 4H), 3.63 (s, 3H), 3.11 (m, 1H), 2.22 (bs, 2H), 2.14 (t, *J* = 6.3 Hz, 2H), 1.58-1.72 (m, 4H), 1.42 (bs, 6H), 1.21 (d, *J* = 6.9 Hz, 6H).

Methyl 10-((2-(2,4-bis(benzyloxy)-5-isopropylbenzoyl) isoindolin-5-yl) amino)-10-oxodecanoate (31)

The title compound **31** was obtained in 73% yield from compound **22** using 10-methoxy-10-oxodecanoic acid in a manner similar to that described for the synthesis of compound **25**; ^{1}H NMR (300 MHz, $CDCl_3$): δ 7.12 -7.47 (m, 14H), 6.48 (s, 1H), 5.11 (s, 4H), 4.89 (bs, 4H), 3.61 (s, 3H), 3.14 (m, 1H), 2.24 (bs, 2H), 2.11 (t, *J* = 6.3 Hz, 2H), 1.57-1.68 (m, 4H), 1.48 (bs, 8H), 1.19 (d, *J* = 6.9 Hz, 6H).

4-((2-(2,4-Bis(benzyloxy)-5-isopropylbenzoyl) isoindolin-5-yl) amino)-4-oxobutanoic acid (32)

A mixture of **25** (0.3 g, 0.49 mmol), aq. LiOH (1M) (3 mL) and dioxane (5 mL) was stirred at 40 °C for 2 h. The reaction was concentrated under reduced pressure and H_2O was added. The mixture was acidified with 3 N HCl and extracted with EtOAc (50 mL x 3). The combined organic layer was dried over anhydrous $MgSO_4$ and concentrated under reduced pressure to yield the acid **32** in 96% yield; ^{1}H NMR (300 MHz, CD_3OD): δ 7.12 - 7.61 (m, 14H), 6.45 (s, 1H), 5.16 (s, 4H), 4.87 (bs, 4H), 3.11 (m, 1H), 2.11 -2.31 (m, 4H), 1.15 (d, *J* = 6.9 Hz, 6H).

5-((2-(2,4-Bis(benzyloxy)-5-isopropylbenzoyl) isoindolin-5-yl) amino)-5-oxopentanoic acid (33)

The title compound **33** was obtained in 92% yield from compound **26** in a manner similar to that described for the synthesis of compound **32**; ^{1}H NMR (300 MHz, CD_3OD): δ 7.18 -7.59 (m, 14H), 6.48 (s, 1H), 5.13 (s, 4H), 4.89 (bs, 4H), 3.22 (m, 1H), 2.12 – 2.24 (m, 4H), 1.99 (m, 2H), 1.12 (d, *J* = 6.9 Hz, 6H).

6-((2-(2,4-Bis(benzyloxy)-5-isopropylbenzoyl) isoindolin-5-yl) amino)-6-oxohexanoic acid (34)

The title compound **34** was obtained in 95% yield from compound **27** in a manner similar to that described for the synthesis of compound **32**; ^{1}H NMR (300 MHz, CD_3OD): 7.19 -7.64 (m, 14H),

6.56 (s, 1H), 5.12 (s, 4H), 4.81 (bs, 4H), 3.09 (m, 1H), 2.21 (t, *J* = 6.9 Hz, 2H), 2.18 (t, *J* = 6.9 Hz, 2H), 1.78-1.85 (m, 4H), 1.21 (d, *J* = 6.9 Hz, 6H).

7-((2-(2,4-Bis(benzyloxy)-5-isopropylbenzoyl) isoindolin-5-yl) amino)-7-oxoheptanoic acid (35)

The title compound **35** was obtained in 93% yield from compound **28** in a manner similar to that described for the synthesis of compound **32**; ^{1}H NMR (300 MHz, CD_3OD): 7.22 -7.67 (m, 14H), 6.49 (s, 1H), 5.12 (s, 4H), 4.76 (bs, 4H), 3.18 (m, 1H), 2.08 – 2.13 (m, 4H), 1.68-1.85 (m, 4H), 1.55 (bs, 2H), 1.15 (d, *J* = 6.9 Hz, 6H).

8-((2-(2,4-Bis(benzyloxy)-5-isopropylbenzoyl) isoindolin-5-yl) amino)-8-oxooctanoic acid (36)

The title compound **36** was obtained in 97% yield from compound **29** in a manner similar to that described for the synthesis of compound **32**; ^{1}H NMR (300 MHz, CD_3OD): 7.12 -7.52 (m, 14H), 6.54 (s, 1H), 5.14 (s, 4H), 4.82 (bs, 4H), 3.11 (m, 1H), 2.20 (bs, 2H), 2.11 (bs, 2H), 1.52-1.67 (m, 4H), 1.43 (bs, 4H), 1.11 (d, *J* = 6.6 Hz, 6H).

9-((2-(2,4-Bis(benzyloxy)-5-isopropylbenzoyl) isoindolin-5-yl) amino)-9-oxononanoic acid (37)

The title compound **37** was obtained in 97% yield from compound **30** in a manner similar to that described for the synthesis of compound **32**; ^{1}H NMR (300 MHz, CD_3OD): 7.13 -7.58 (m, 14H), 6.47 (s, 1H), 5.09 (s, 4H), 4.89 (bs, 4H), 3.18 (m, 1H), 2.22 (bs, 2H), 2.14 (bs, 2H), 1.59-1.73 (m, 4H), 1.48 (bs, 6H), 1.17 (d, *J* = 6.9 Hz, 6H).

10-((2-(2,4-Bis(benzyloxy)-5-isopropylbenzoyl) isoindolin-5-yl) amino)-10-oxodecanoic acid (38)

The title compound **38** was obtained in 91% yield from compound **31** in a manner similar to that described for the synthesis of compound **32**; ^{1}H NMR (300 MHz, CD_3OD): ^{1}H NMR (300 MHz,

CD_3OD): 7.21 -7.52 (m, 14H), 6.49 (s, 1H), 5.05 (s, 4H), 4.82 (bs, 4H), 3.13 (m, 1H), 2.13 - 2.21 (m, 4H), 1.61-1.71 (m, 4H), 1.42 (bs, 8H), 1.19 (d, *J* = 6.9 Hz, 6H).

N^1-(Benzyloxy)-N^4-(2-(2,4-bis(benzyloxy)-5-isopropylbenzoyl) isoindolin-5-yl) succinamide (39)

The title compound **39** was obtained in 82% yield from compound **32** using $NH_2OBn.HCl$ in a manner similar to that described for the synthesis of compound **25**. ^1H NMR (300 MHz, CD_3OD): 7.14 - 7.56 (m, 19H), 6.41 (s, 1H), 5.21 (s, 2H), 5.18 (s, 4H), 4.81 (s, 4H), 3.12 (m, 1H), 2.41-2.44 (m, 4H), 1.21 (d, *J* = 6.9 Hz, 6H).

N^1-(Benzyloxy)-N^5-(2-(2,4-bis(benzyloxy)-5-isopropylbenzoyl) isoindolin-5-yl) glutaramide (40)

The title compound **40** was obtained in 73% yield from compound **33** using $NH_2OBn.HCl$ in a manner similar to that described for the synthesis of compound **25**. ^1H NMR (300 MHz, CD_3OD): 7.12 - 7.54 (m, 19H), 6.49 (s, 1H), 5.19 (s, 2H), 5.14 (s, 4H), 4.89 (s, 4H), 3.16 (m, 1H), 2.21-2.24 (m, 4H), 1.91 (m, 2H), 1.16 (d, *J* = 6.9 Hz, 6H).

N^1-(Benzyloxy)-N^6-(2-(2,4-bis(benzyloxy)-5-isopropylbenzoyl) isoindolin-5-yl)adipamide (41)

The title compound **41** was obtained in 77% yield from compound **34** using $NH_2OBn.HCl$ in a manner similar to that described for the synthesis of compound **25**. ^1H NMR (300 MHz, CD_3OD): 7.15 - 7.48 (m, 19H), 6.45 (s, 1H), 5.12 (s, 2H), 5.03 (s, 4H), 4.81 (s, 4H), 3.09 (m, 1H), 2.22-2.29 (m, 4H), 1.78-1.85 (m, 4H), 1.15 (d, *J* = 6.9 Hz, 6H).

N^1-(Benzyloxy)-N^7-(2-(2,4-bis(benzyloxy)-5-isopropylbenzoyl) isoindolin-5-yl) heptanediamide (42)

The title compound **42** was obtained in 71% yield from compound **35** using $NH_2OBn.HCl$ in a manner similar to that described for the synthesis of compound **25**. ^1H NMR (300 MHz, CD_3OD):

7.17 - 7.49 (m, 19H), 6.49 (s, 1H), 5.17 (s, 2H), 5.09 (s, 4H), 4.85 (s, 4H), 3.11 (m, 1H), 2.21-2.32 (m, 4H), 1.68-1.85 (m, 4H), 1.55 (bs, 2H), 1.15 (d, *J* = 6.9 Hz, 6H).

***N*^{1}-(Benzyloxy)-*N*^{8}-(2-(2,4-bis(benzyloxy)-5-isopropylbenzoyl) isoindolin-5-yl) octanediamide (43)**

The title compound **43** was obtained in 76% yield from compound **36** using $NH_2OBn.HCl$ in a manner similar to that described for the synthesis of compound **25.** ^{1}H NMR (300 MHz, CD_3OD): 7.12 - 7.41 (m, 19H), 6.41 (s, 1H), 5.11 (s, 2H), 5.02 (s, 4H), 4.81 (s, 4H), 3.09 (m, 1H), 2.11 - 2.22 (m, 4H), 1.61-1.82 (m, 4H), 1.54 (bs, 4H), 1.15 (d, *J* = 6.9 Hz, 6H).

***N*^{1}-(Benzyloxy)-*N*^{9}-(2-(2,4-bis(benzyloxy)-5-isopropylbenzoyl) isoindolin-5-yl) nonane-diamide (44)**

The title compound **44** was obtained in 73% yield from compound **37** using $NH_2OBn.HCl$ in a manner similar to that described for the synthesis of compound **25.** ^{1}H NMR (300 MHz, CD_3OD): 7.14 - 7.45 (m, 19H), 6.48 (s, 1H), 5.17 (s, 2H), 5.12 (s, 4H), 4.88 (s, 4H), 3.11 (m, 1H), 2.13 - 2.25 (m, 4H), 1.61-1.82 (m, 4H), 1.47 (bs, 6H), 1.15 (d, *J* = 6.9 Hz, 6H).

***N*^{1}-(Benzyloxy)-*N*^{10}-(2-(2,4-bis(benzyloxy)-5-isopropylbenzoyl) isoindolin-5-yl) decane-diamide (45)**

The title compound **45** was obtained in 82% yield from compound **38** using $NH_2OBn.HCl$ in a manner similar to that described for the synthesis of compound **25.** ^{1}H NMR (300 MHz, CD_3OD): 7.18 - 7.52 (m, 19H), 6.42 (s, 1H), 5.12 (s, 2H), 5.02 (s, 4H), 4.85 (s, 4H), 3.05 (m, 1H), 2.23 - 2.25 (m, 4H), 1.68-1.79 (m, 4H), 1.49 (bs, 6H), 1.21 (d, *J* = 6.9 Hz, 6H).

***N*^{1}-(2-(2,4-Dihydroxy-5-isopropylbenzoyl) isoindolin-5-yl)-*N*^{4}-hydroxysuccinamide (11)**

A catalytic amount of 10% palladium on carbon was added to the solution of compound **39 (**0. 2 g, 0.286 mmol) in MeOH (10 mL), and the reaction mixture was stirred for 2 h under H_2. The

reaction mixture was filtered over celite and the filtrate was dried in vacuum and purified by silica gel chromatography (EtOAc) to give **11** in 70% yield. HPLC purity: 97.62 %; mp: 111-112 °C; ^{1}H NMR (300 MHz, DMSO-d_6): 10.43 (s, 1H), 10.08 (s, 1H), 10.01 (s, 1H), 9.62 (s, 1H), 8.72 (s, 1H), 7.61 (m, 1H), 7.42 (bs, 1H), 7.21 (d, *J* = 6.6 Hz, 1H), 7.06 (s, 1H), 6.41 (s, 1H), 4.74 (d, *J* = 11.1 Hz, 4H), 3.11 (m, 1H), 2.30 (t, *J* = 6.9 Hz, 2H), 2.00 (t, *J* = 7.5 Hz, 2H), 1.15 (d, *J* = 6.9 Hz, 6H); ^{13}C NMR (75 MHz, DMSO-d_6) : 168.56, 166.61, 166.55, 154.62, 151.70, 136.49, 123.47, 123.26, 120.75, 116.31, 111.67, 111.164, 100.33, 33.42, 29.44, 23.75, 20.47, 18.98. HRMS (ESI) for $C_{22}H_{24}N_3O_6$ $(M-H)^-$: calcd, 426.1665; found, 426.1663.

N^1-(2-(2,4-Dihydroxy-5-isopropylbenzoyl) isoindolin-5-yl)-N^5-hydroxyglutaramide (12)

The title compound **12** was obtained in 72% yield from compound **40** in a manner similar to that described for the synthesis of compound **11**. HPLC purity: 98.95 %; mp: 115-116 °C; ^{1}H NMR (300 MHz, DMSO-d_6): 10.40 (s, 1H), 10.08 (s, 1H), 9.95 (s, 1H), 9.62 (s, 1H), 8.70 (s, 1H), 7.65 (m, 1H), 7.42 (bs, 1H), 7.24 (bs, 1H), 7.06 (s, 1H), 6.41 (s, 1H), 4.75 (d, *J* = 12.6 Hz, 4H), 3.11 (m, 1H), 2.32 (t, *J* = 6.9 Hz, 2H), 2.04 (bs, 2H), 1.81 (m, 2H), 1.15 (d, *J* = 6.9 Hz, 6H); ^{13}C NMR (75 MHz, DMSO-d_6) : 171.20, 169.26, 169.20, 157.26, 154.36, 139.14, 126.13, 125.90, 123.39, 118.96, 114.31, 113.80, 102.97, 36.08, 32.09, 26.40, 23.13, 21.63; HRMS (ESI) for $C_{23}H_{28}N_3O_6$ $(M + H^+)$: calcd, 442.1978; found, 442.1982.

N^1-(2-(2, 4-Dihydroxy-5-isopropylbenzoyl) isoindolin-5-yl) -N^6-hydroxyadipamide (13)

The title compound **13** was obtained in 75% yield from compound **41** in a manner similar to that described for the synthesis of compound **11**. HPLC purity: 97.53%; mp: 124-125 °C; ^{1}H NMR (300 MHz, CD_3OD): 7.61 (bs, 1H), 7.43 (d, *J* = 8.4 Hz, 1H), 7.27 (bs, 1H), 7.20 (s, 1H), 6.40 (s, 1H), 4.89 (s, 4H), 3.22 (m, 1H), 2.41 (bs, 2H), 2.13 (bs, 4H), 1.65-1.72 (m, 4H), 1.24 (d, *J* = 6.9 Hz, 6H); 13C NMR (75 MHz, CD_3OD) : 173.23, 157.67, 154.401, 138.234, 126.60, 125.53,

122.59, 119.49, 114.09, 113.02, 102.26, 36.46, 28.52, 26.32, 25.19, 21.73; HRMS (ESI) for $C_{24}H_{28}N_3O_6$ $(M - H)^-$: calcd, 454.1978; found, 454.1972

N^1-(2-(2,4-Dihydroxy-5-isopropylbenzoyl) isoindolin-5-yl) -N^7-hydroxyheptanediamide (14)

The title compound **14** was obtained in 75% yield from compound **42** in a manner similar to that described for the synthesis of compound **11**. HPLC purity: 97.25%; mp: 201 - 202 °C; ^{1}H NMR (300 MHz, DMSO-d_6): 10.36 (s, 1H), 10.13 (s, 1H), 9.91 (s, 1H), 9.65 (bs, 1H), 8.69 (s, 1H), 7.68 (bs, 1H), 7.43 (d, *J* = 7.5 Hz, 1H), 7.27 (bs, 1H), 7.08 (s, 1H), 6.42 (s, 1H), 4.74 (d, *J* = 12.3 Hz, 4H), 3.14 (m, 1H), 2.30 (t, *J* = 7.2 Hz, 2H), 1.95 (t, *J* = 7.5 Hz, 2H), 1.47-1.59 (m, 4H), 1.27 (bs, 2H), 1.15 (d, *J* = 6.6 Hz, 6H); ^{13}C NMR (125 MHz, DMSO-d_6) : 171.13, 169.05, 168.74, 156.77, 153.96, 138.66, 129.57, 125.59, 125.38, 122.82, 118.44, 113.68, 113.28, 102.49, 39.92, 32.20, 29.22, 25.89, 24.96, 22.02; HRMS (ESI) for $C_{25}H_{30}N_3O_6$ $(M - H)^-$: calcd, 468.2135; found, 468.2135.

N^1-(2-(2,4-Dihydroxy-5-isopropylbenzoyl) isoindolin-5-yl) -N^8-hydroxyoctanediamide (15)

The title compound **15** was obtained in 78% yield from compound **43** in a manner similar to that described for the synthesis of compound **11**. HPLC purity: 98.12%; mp: 177-178 °C; ^{1}H NMR (300 MHz, DMSO-d_6): 10.35 (s, 1H), 10.09 (s, 1H), 9.91 (s, 1H), 9.63 (s, 1H), 8.67 (s, 1H), 7.70 (m, 1H), 7.42 (bs, 1H), 7.24 (bs, 1H), 7.06 (s, 1H), 6.41 (s, 1H), 4.77 (s, 4H), 3.11 (m, 1H), 2.30 (bs, 2H), 1.95 (t, *J* = 6.3 Hz, 2H), 1.58-1.61 (m, 4H), 1.28 (bs, 4H), 1.15 (d, *J* = 6.6 Hz, 6H); ^{13}C NMR (75 MHz, DMSO-d_6) : 174.17, 171.54, 170.74, 160.16, 158.61, 139.12, 126.55, 125.58, 122.73, 118.86, 113.49, 109.08, 103.004, 36.84, 33.40, 26.53, 25.39, 24.76, 22.20; HRMS (ESI) for $C_{26}H_{32}N_3O_6$ $(M - H)^+$: calcd, 482.2291; found, 482.2294.

N^1-(2-(2,4-Dihydroxy-5-isopropylbenzoyl) isoindolin-5-yl)-N^9-hydroxynonanediamide (16)

The title compound **16** was obtained in 71% yield from compound **44** in a manner similar to that described for the synthesis of compound **11**. HPLC purity: 98.88 %; mp: 126-127 °C; ^{1}H NMR (300 MHz, CD_3OD) : 7.61 (s, 1H), 7.43 (d, *J* = 8.1 Hz, 1H), 7.26 (bs, 1H), 7.20 (s, 1H), 6.40 (s, 1H), 4.89 (s, 4H), 3.22 (m, 1H), 2.38 (d, *J* = 7.5 Hz, 2H), 2.30 (t, *J* = 7.5 Hz, 2H), 1.60-1.74 (m, 4H), 1.40 (bs, 6H), 1.23 (d, *J* = 6.9 Hz, 6H); ^{13}C NMR (125 MHz, DMSO-d_6): 174.38, 171.15, 168.74, 156.77, 138.66, 125.60, 125.38, 122.82, 118.43, 113.28, 102.49, 36.31, 33.59, 28.52, 25.89, 25.02, 24.41, 22.59; HRMS (ESI) for $C_{27}H_{34}N_3O_6$ $(M - H)^-$: calcd, 496.2448; found, 496.2447.

N^1-(2-(2,4-Dihydroxy-5-isopropylbenzoyl)isoindolin-5-yl)-N^{10}-hydroxydecanediamide (17)

The title compound **17** was obtained in 75% yield from compound **45** in a manner similar to that described for the synthesis of compound **11**. HPLC purity: 97.54 %; mp: 125-126 °C; ^{1}H NMR (300 MHz, DMSO-d_6): 10.36 (s, 1H), 10.13 (s, 1H), 9.91 (s, 1H), 9.65 (bs, 1H), 8.69 (s, 1H), 7.68 (bs, 1H), 7.43 (d, *J* = 7.5 Hz, 1H), 7.27 (bs, 1H), 7.08 (s, 1H), 6.42 (s, 1H), 4.74 (d, *J* = 12.3 Hz, 4H), 3.14 (m, 1H), 2.30 (t, *J* = 7.2 Hz, 2H), 1.95 (t, *J* = 7.5 Hz, 2H), 1.47-1.59 (m, 4H), 1.27 (bs, 4H), 1.15 (d, *J* = 6.6 Hz, 6H); ^{13}C NMR (75 Hz, DMSO-d_6): 169.09, 167.01, 166.66, 154.66, 151.79, 136.53, 123.46, 123.27, 120.72, 116.30, 111.57, 111.14, 100.34, 34.21, 30.07, 26.55, 26.47, 26.38, 22.92, 20.45; HRMS (ESI) for $C_{28}H_{36}N_3O_6$ (M - H): calcd, 510.2604; found, 510.2605.

5-Bromo-isoindoline (47)

Sodium borohydride (3.48 g, 92.0 mmol) was added to the solution of 5-bromopthalamide (2.0 g, 8.8 mmol) in THF, and the resultant suspension was cooled to -10 °C. Then, $BF_3.Et_2O$ (12.7 mL, 102.6 mmol) was added slowly and the reaction mixture was refluxed. After 24 h, the reaction mixture was allowed to cool to 0 °C and cold H_2O (18 mL) was added. EtOAc (100 ml) was

added and the reaction mixture was made alkaline using 6.0 M aqueous NaOH. The organic layer was separated and concentrated using a rotary evaporator. The residue was diluted with Et_2O (50 mL) and acidified to pH 2. The aqueous layer was separated, made alkaline to pH 10 using 6.0 M aqueous NaOH and extracted with EtOAc (70 mL). The organic layer was separated, washed with brine (3 × 70 mL), dried (Na_2SO_4) and concentrated using rotary evaporator to yied the 5-bromo-isoindoline (**47**). The residue was used in further reactions without purification.

(2,4-Bis-benzyloxy-5-isopropyl-phenyl)-(5-bromo-1,3-dihydro-isoindol-2-yl)-methanone (48)

The title compound **48** was obtained in 75% yield from compound **47** in a manner similar to that described for the synthesis of compound **21**; ^{1}H NMR (300 MHz, $CDCl_3$) : 7.38 – 7.50 (m, 7H), 7.23-7.33 (s, 7H), 6.60 (s, 1H), 5.10 (s, 2H), 5.08 (s, 2H), 4.97 (d, *J* = 13. 2 Hz, 2H), 4.62 (d, *J* = 10.2 Hz, 2H), 3.35 (m, 1H), 1.24 (d, *J* = 6.9 Hz, 6H).

3-[2-(2,4-Bis-benzyloxy-5-isopropyl-benzoyl)-2,3-dihydro-1H-isoindol-5-yl]-acrylic acid methyl ester (49)

A mixture of **48** (1 g, 2.65 mmol), palladium(II) acetate (0.119 g, 0.53 mmol), triphenylphosphine (0.278 g, 1.06 mmol), TEA (1.10 mL, 7.95 mmol) and methyl acrylate (0.288 mL, 3.18 mmol) in DMF (5 mL) was stirred at 100 °C for 12 h. The reaction was quenched with H_2O, and extracted with EtOAc (50 mL x 3). The combined organic layer was dried over anhydrous $MgSO_4$ and concentrated under reduced pressure. The resulting residue was purified by silica gel chromatography (EtOAc) to give compound **49** in 53% yield; 1H NMR (300 MHz, CD_3OD) : 7.41 – 7.73 (m, 8H), 7.08 – 7.37 (m, 7H), 6.85 (s, 1H), 6.52 (d, *J* = 15.6 Hz, 1 H), 5.17 (s, 2H), 5.14 (s, 2H), 4.97 (bs, 2H), 4.62 (bs, 2H), 3.80 (s, 3H), 3.35 (m, 1H), 1.23 (d, *J* = 6.9 Hz, 6H).

3-[2-(2,4-Dihydroxy-5-isopropyl-benzoyl)-2,3-dihydro-1H-isoindol-5-yl]-N-hydroxy-acrylamide (18)

The compound **49** was subjected to hydrolysis using lithium hydroxide followed by EDC/HOBt mediated amidation with NH_2OBn. The residue (0.5 g, 0.76 mmol) obtained after purification was dissolved in DCM and BCl_3 (1 M in heptane, 6 eq) was added to the solution at 0 °C. The reaction mixture was stirred for 45 min at the same temperature. The reaction mixture was filtered to collect the solid precipitated solid (**18**, 66% yield). HPLC purity: 95.18%; mp: 131-133 °C; ^{1}H NMR (300 MHz, DMSO-d_6) : 10.77 (s, 1H), 10.06 (s, 1H), 9.63 (s, 1H), 9.06 (s, 1H), 7.40 – 7.57 (m, 4H), 7.06 (s, 1H), 6.42-6.49 (m, 2H), 4.80 (s, 4H), 3.11 (m, 1H), 1.15 (d, *J* = 6.9 Hz, 6H); ^{13}C NMR (75 MHz, DMSO-d6): 171.05, 164.80, 158.09, 154.39, 140.10, 134.56, 128.21, 127.58, 127.29, 126.83, 125.63, 122.92, 121.59, 116.88, 112.12, 102.30, 26.36, 22.12, 21.718; HRMS (ESI) for $C_{21}H_{23}N_2O_5$ (M + H)+ : calcd, 383.1607; found, 383.1608.

4.2 Biology

4.2.1 Cell culture

All human cancer cells were maintained in RPMI 1640 medium containing 10% fetal bovine serum, 100 units/mL penicillin, 100 mg/mL streptomycin and 2.5 mg/mL amphotericin B. Cells were cultured in tissue culture flasks in a humidified incubator at 37 °C, in an atmosphere of 5% CO_2 and 95% air.

4.2.2 Sulforhodamine B (SRB) assays

Counted cells were seeded in 96-well plates in medium with 5% FBS. After 24 h, cells were fixed with 10% trichloroacetic acid (TCA) to represent the cell population at the time of compound addition (T0). After additional incubation of DMSO or test compound for 48 h, cells were fixed with 10% TCA and then stained with SRB at 0.4% (w/ v) in 1% AcOH. Unbound SRB was washed out with 1% AcOH and SRB-containing cells were solubilized with 10 mMTrizma

base. The absorbance was read at a wavelength of 515 nm. Using the subsequent absorbance measurements, such as time zero (T0), control growth (C), and cell growth in the presence of the compound (Tx), the percentage of growth was calculated at each of the compound concentration levels. Growth inhibition of 50% (GI_{50}) was calculated from the equation [(TieTz)/(CeTz)] _ 100 ¼ 50, which provides the compound concentration resulting in a 50% reduction in the net protein increase (as measured by SRB staining) in control cells during the incubation with the compound.

4.2.3 HeLa nuclear extract HDAC activity assay

HDAC Fluorescent Activity Assay Kit (BioVision, CA) was used to detect HeLa nuclear extract HDAC activity according to the manufacturer's instructions. Briefly, the HDAC fluorometric substrate and assay buffer were added to HeLa nuclear extracts in a 96-well format and incubated at 37 °C for 30 min. The reaction was stopped by adding lysine developer, and the mixture was incubated for a further 30 min at 37 °C. Additional negative controls included incubation without the nuclear extract, without the substrate, or without both. A fluorescence plate reader with excitation at 355 nm and emission at 460 nm was used to quantify the HDAC activity.

4.2.4 HDAC enzymes inhibition assays

Enzyme inhibition assays were performed by the Reaction Biology Corporation, Malvern, PA. (http://www.reactionbiology.com). The substrate for HDAC1, -3, -6 and -8 was a fluorogenic peptide derived from p53 residues 379–382 [RHKK(Ac)]. Compounds were dissolved in DMSO and tested in 10-dose IC_{50} mode with 3-fold serial dilution starting at 10 μM. Trichostatin A (TSA) was the reference.

4.2.5 Western blot analysis

Cell lysates were prepared, and proteins were separated by 7.5–15% SDS-PAGE, transferred onto a PVDF membrane, and then immunoblotted with specific antibodies. Proteins were visualized with an ECL detection system. Compound tested in a 10-dose IC_{50} with 3-fold serial dilution starting at 10 μM.

4.2.6 FACScan Flow Cytometric analysis

Cells were seeded in 6-well plates (2.5×10^5/well) and incubated overnight. Next day cells were treated with DMSO or indicated compounds at various concentrations for 48 h. Cells were washed with phosphate-buffered saline, fixed in ice-cold 70% EtOH at -20 °C overnight, and stained with propidium iodide (80 ug/ml) containing Triton X-100 (0.1%, v/v) and RNase A (100 ug/ml) in phosphate-buffered saline. DNA content was counted and analyzed with the FACScan and CellQuest software (Becton Dickinson, Mountain View, CA, USA).

4.2.7 Docking study

Docking analysis was performed using the molecular docking software, LeadIT[49]. The crystal structures of HSP90 (PDB ID: 2CCU), HDAC6 (PDB ID: 5EDU), HDAC1 (PDB ID: 5ICN) and HDAC3 (PDB ID: 4A69) were downloaded from the Protein Data Bank[50]. The LeadIT software was used to prepare the protein structures. Water molecules as well as the co-crystal ligand were removed. The binding site of each structure was determined at a radius of 15 Å from the co-crystallized ligand. For compound **10** analysis a water molecule was added to the HDAC6 catalytic site due to its monodentate binding to Zn^{2+}. Because the human HDAC6 co-crystal structure does not contain water molecules in the catalytic site. Therefore water molecules were taken from the *Danio rerio* HDAC6 co-crystal structure (PDB ID: 5EF7). The docking strategy used an enthalpy and entropy approach. Scoring parameters used default settings. The maximum solutions for each iteration and each fragmentation was set to 500.

4.2.8 *In vivo* study

All animal studies were conducted in accordance with the guidelines of the Animal Care and Use Committee at Taipei Medical University (IACUC No.: LAC-2016-0374). H1975 cells (1 x 10^7 cells/mice) were inoculated subcutaneously in balb/c male *nu/nu* mice (5-6 weeks). Once the tumor size was approximately 100 mm^3, mice were allocated at random to treatment groups: Control group (vehicle; 5% DMSO/5% Cremophor in D5W); 50 or 100 mg/kg of compound **17** once a day (qd) by intraperitoneal injection; 20 mg/kg of afatinib was given orally to mice every day as positive control. Caliper measurements were used to calculate tumor volume (V, mm^3) using the formula $V=lw^2/2$, with l being the length and the w being the width of the tumor. During the experiment, the tumor size and body weight were measured twice each week. Tumor growth inhibition (TGI) was calculated by dividing the tumor volumes from treatment groups by those of the control groups as 100%.

4.2.9 Western blot analysis (PD-L1 expression in IFN-γ treated H1975 cells)

Cells were lysed with RIPA lysis buffer containing protease inhibitor cocktail. The cell lysates were separated in a 10% reducing gel by sodium dodecyl sulfate polyacrylamide gel electrophoresis (SDS-PAGE) and transferred onto a nitrocellulose membrane. The blots were incubated with mouse anti-PDL-1 antibody (Cat#AW5698;ABGENT, San Diego, California, U.S.A.) or mouse anti-β-actin antibody (Cat# A5416; Sigma-Aldrich, St. Louis, MO, U.S.A.) for 1h. HRP-conjugated goat anti-mouse IgG antibodies (1 μg/ml; Cat# 115-035-003; Jackson ImmunoResearch Laboratories, West Grove, PA, U.S.A.) and enhanced chemiluminescence (ECL) substrate (Thermo Fisher Scientific, Waltham, MA, U.S.A.) were used to detect protein signals.

4.2.10 Analysis of PD-L1 expression on cell surface by flow cytometry

Cells suspended at a cell number of 3 x 10^5 cells/tube were wash in PBS buffer containing 0.05% (w/v) BSA (PBS/BSA) and then incubated with 5 μg/ml of mouse anti-PDL-1 antibody (Cat# 14-5983-82; Thermo Fisher Scientific) for 1h. Then cells were incubated with FITC-conjugated goat anti-mouse IgG antibody (Cat# 115-096-071; Jackson ImmunoResearch Laboratories) for 1h. After the removal of unbound antibodies by extensive washing with PBS/BSA, FITC fluorescence of the cells were measured by FACScan flow cytometer (BD Biosciences, San Jose, CA, USA). The data and mean fluorescence intensity (MFI) of FITC signal were analyzed by CellQuest software (BD Biosciences, San Jose, CA, USA).

Acknowledgment. This research were supported by the Ministry of Science and Technology, Taiwan (grant no. MOST 107-2113-M-038-001).

ABBREVIATIONS USED

HDAC6, histone deacetylase 6; HSP90, heat shock protein 90; DCM, dichloromethane; DIPEA, diisopropylethylamine; TEA, trimethylamine; EDC·HCl, *N*-(3-Dimethylaminopropyl)-*N′*-ethylcarbodiimide hydrochloride; HOBt, Hydroxybenzotriazole.

Reference

1. Siegel, R. L.; Miller, K. D.; Jemal, A. Cancer statistics, 2019. *CA Cancer J Clin.* **2019** 69, 7-34.
2. Pillai, R.; Fennell, D.; Kovcin, V.; Ciuleanu, T.; Ramlau, R.; Kowalski, D.; Schenker, M.; Perin, B.; Yalcin, I.; Teofilovici, F.; Vukovic, V.; Ramalingam, S. PL03.09: Phase 3 study of ganetespib, a heat shock protein 90 inhibitor, with docetaxel versus docetaxel in advanced non-small cell lung cancer (GALAXY-2). *J. Thorac. Oncol.* **2017**, *12*, S7–S8.
3. Nagaraju, G. P.; Park, W.; Wen, J.; Mahaseth, H.; Landry, J.; Farris, A. B.; Willingham, F.; Sullivan, P. S.; Proia, D. A.; El-Hariry, I.; Taliaferro-Smith, L.; Diaz, R.; El-Rayes, B. F. Antiangiogenic effects of ganetespib in colorectal cancer mediated through inhibition of HIF-1alpha and STAT-3. *Angiogenesis* **2013**, *16*, 903–917.
4. Damaskos, C.; Tomos, I.; Garmpis, N.; Karakatsani, A.; Dimitroulis, D.; Garmpi, A.; Spartalis, E.; Kampolis, C. F.; Tsagkari, E.; Loukeri, A. A.; Margonis, G. A.; Spartalis, M.; Andreatos, N.; Schizas, D.; Kokkineli, S.; Antoniou, E. A.; Nonni, A.; Tsourouflis, G.; Markatos, K.; Kontzoglou, K.; Kostakis, A.; Tomos, P. Histone Deacetylase Inhibitors as a Novel Targeted Therapy Against Non-small Cell Lung Cancer: Where Are We Now and What Should We Expect? *Anticancer Res.* **2018**, *38*, 37-43.
5. Gridelli, C. R.; Antonio, R.; Paolo, M. The potential role of histone deacetylase inhibitors in the treatment of non-small-cell lung cancer. *Crit. Rev. Onc. Hematol.* **2008,** *68*, 29–36.
6. Shaw, A. T.; Kim, D. W.; Nakagawa, K.; Seto, T.; Crinó, L.; Ahn, M. J.; De Pas, T.; Besse, B.; Solomon, B. J.; Blackhall, F.; Wu, Y. L.; Thomas, M.; O'Byrne, K. J.; Moro-Sibilot, D.; Camidge, D. R.; Mok, T.; Hirsh, V.; Riely, G. J.; Iyer, S.; Tassell, V.; Polli, A.; Wilner, K. D.;

Jänne, P. A.; Crizotinib versus chemotherapy in advanced ALK-positive lung cancer. *N. Engl. J. Med.* **2013**, *368*, 2385–2394.

7. Rosell, R.; Carcereny, E.; Gervais, R.; Vergnenegre, A.; Massuti, B.; Felip, E.; Palmero, R.; Garcia-Gomez, R.; Pallares, C.; Sanchez, J. M.; Porta, R.; Cobo, M.; Garrido, P.; Longo, F.; Moran, T.; Insa, A.; De Marinis, F.; Corre, R.; Bover, I.; Illiano, A.; Dansin, E.; de Castro, J.; Milella, M.; Reguart, N.; Altavilla, G.; Jimenez, U.; Provencio, M.; Moreno, M. A.; Terrasa, T.; Muñoz-Langa, J.; Valdivia, J.; Isla, D.; Domine, M.; Molinier, O.; Mazieres, J.; Baize, N.; Garcia-Campelo, R.; Robinet, G.; Rodriguez-Abreu, D.; Lopez-Vivanco, G.; Gebbia, V.; Ferrera-Delgado, L.; Bombaron, P.; Bernabe, R.; Bearz, A.; Artal, A.; Cortesi, E.; Rolfo, C.; Sanchez-Ronco, M.; Drozdowskyj, A.; Queralt, C.; Aguirre, I.D.; Ramirez, J. L.; Sanchez, J. J.; Molina, M. A.; Taron, M.; Paz-Ares, L. Erlotinib versus standard chemotherapy as first-line treatment for European patients with advanced EGFR mutation-positive non-small-cell lung cancer (EURTAC): a multicentre, open-label, randomised phase 3 trial. *Lancet Oncol.* **2012**, *13*, 239–246.
8. Marson, C. M. Histone deacetylase inhibitors: design, structure-activity relationships and therapeutic implications for cancer. *Anticancer Agents Med. Chem.* **2009**, *9*, 661−692.
9. Minucci, S.; Pelicci, G. Histone deacetylase inhibitors and the promise of epigenetic (and more) treatment for cancer. *Nat. Rev. Cancer* **2006**, *6*, 38−51.
10. Komatsu, N.; Kawamata, N.; Takeuchi, S.; Yin, D.; Chien, W.; Miller, C. W.; Koeffler, H. P. SAHA, a HDAC inhibitor, has profound anti-growth activity against non-small cell lung cancer cells. *Oncol. Rep.* **2006**, *15*, 187-191.
11. Ong, P. S.; Wang, L.; Chia, D. M.; Seah, J. Y.; Kong, L. R.; Thuya, W. L.; Chinnathambi, A.; Lau, J. Y.; Wong, A. L.; Yong, W. P.; Yang, D.; Ho, P. C.; Sethi, G.; Goh, B. C. A novel

combinatorial strategy using Seliciclib (®) and Belinostat (®) for eradication of non-small cell lung cancer *via* apoptosis induction and BID activation. *Cancer Lett.* **2016**, *381*, 49-57.

12. Greve, G.; Schiffmann, I.; Pfeifer, D.; Pantic, M.; Schüler, J.; Lübbert, M. The pan-HDAC inhibitor panobinostat acts as a sensitizer for erlotinib activity in *EGFR*-mutated and –wildtype non-small cell lung cancer cells. *BMC Cancer* **2015**, *15,* 947.
13. Chen, J. H.; Zheng, Y. L.; Xu, C. Q.; Gu, L. Z.; Ding, Z. L.; Qin, L.; Wang, Y.; Fu, R.; Wan, Y. F.; Hu, C. P. Valproic acid (VPA) enhances cisplatin sensitivity of non-small cell lung cancer cells *via* HDAC2 mediated down-regulation of ABCA1. *Biol. Chem.* **2016**, *398,* 785-792.
14. Gavrilov, V.; Lavrenkov, K.; Ariad, S.; Shany, S. Sodium valproate, a histone deacetylase inhibitor, enhances the efficacy of vinorelbine-cisplatin-based chemoradiation in non-small cell lung cancer cells. *Anticancer Res.* **2014**, *34*, 6565-6572.
15. Bao, L.; Diao, H.; Dong, N.; Su, X.; Wang, B.; Mo, Q.; Yu, H.; Wang, X.; Chen, C. Histone deacetylase inhibitor induces cell apoptosis and cycle arrest in lung cancer cells via mitochondrial injury and p53 up-acetylation. *Cell Biol. Toxicol*. **2016**, *32*, 469–482.
16. McLaughlin, K. A.; Nemeth, Z.; Bradley, C. A.; Humphreys, L.; Stasik, I.; Fenning, C.; Majkut, J.; Higgins, C.; Crawford, N.; Holohan, C.; Johnston, P. G.; Harrison, T.; Hanna, G. G.; Butterworth, K. T.; Prise, K. M.; Longley, D. B. FLIP: A targetable mediator of resistance to radiation in non-small cell lung cancer. *Mol. Cancer Ther*. **2016**, *15*, 2432-2441.
17. Ramalingam, S. S.; Maitland, M. L.; Frankel, P.; Argiris, A. E.; Koczywas, M.; Gitlitz, B.; Thomas, S.; Espinoza-Delgado, I.; Vokes, E. E.; Gandara, D. R.; Belani, C. P. Carboplatin and paclitaxel in combination with either vorinostat or placebo for first-line therapy of advanced non–small-cell lung cancer. *J. Clin. Oncol*. **2010**, *28*, 56-62.

18. Owonikoko, T. K.; Ramalingam, S. S.; Kanterewicz, B.; Balius, T. E. Belani, C. P.; Hershberger, P. A. Vorinostat increases carboplatin and paclitaxel activity in non-small cell lung cancer cells. *Int. J. Cancer* **2010**, *126*, 743-755.
19. Traynor, A. W.; Dubey, S.; Eickhoff, J. C.; Kolesar, J. M.; Schell, K.; Huie, M. S.; Groteluschen, D. L.; Marcotte, S. M.; Hallahan, C. M.; Weeks, H. R.; Wilding, G.; Espinoza-Delgado, I.; Schiller, J. H. Vorinostat (NSC# 701852) in patients with relapsed non-small cell lung cancer: a Wisconsin Oncology Network phase II study. *J. Thorac. Oncol.* **2009**, *4*, 522-526.
20. McLaughlin, K. A.; Nemeth, Z.; Bradley, C. A.; Humphreys, L.; Stasik, I.; Fenning, C.; Majkut, J.; Higgins, C.; Crawford, N.; Holohan, C.; Johnston, P. G.; Harrison, T.; Hanna, G. G.; Butterworth, K. T.; Prise, K. M.; Longley, D. B. FLIP: A targetable mediator of resistance to radiation in non-small cell lung cancer. *Mol Cancer Ther*. **2016**, *15*, 2432-2441.
21. Pillai, R. N.; Ramalingam, S. S. Heat shock protein 90 inhibitors in non-small-cell lung cancer, *Curr. Opin. Oncol.* **2014**, *26*, 159–164.
22. Chatterjee, S.; Bhattacharya, S.; Socinski, M. A.; Burns, T. F. HSP90 inhibitors in lung cancer: promise still unfulfilled, *Clin. Adv. Hematol. Oncol*. **2016**, *14*, 346-56.
23. Sequist, L. V.; Gettinger, S.; Senzer, N. N.; Martins, R. G.; Jänne, P. A.; Lilenbaum, R.; Gray, J.E.; Iafrate, A. J.; Katayama, R.; Hafeez, N.; Sweeney, J. ; Walker, J. R.; Fritz, C.; Ross, R.W.; Grayzel, D. ; Engelman, J. A.; Borger, D. R.; Paez, G.; R. Natale. Activity of IPI-504, a novel heat-shock protein 90 inhibitor, in patients with molecularly defined non-small-cell lung cancer, *J. Clin. Oncol.* **2010**, *28*, 4953-4960.
24. Kasibhatla, S. R.; Hong, K.; Biamonte, M. A.; Busch DJ, Karjian, P. L.; Sensintaffar, J. L.; Kamal, A.; Lough, R. E.; Brekken, J.; Lundgren, K.; Grecko, R.; Timony, G. A.; Ran, Y.;

Mansfield, R.; Fritz, L. C.; Ulm, E.; Burrows, F. J.; Boehm, M. F. Rationally designed high-affinity 2-amino-6-halopurine heat shock protein 90 inhibitors that exhibit potent antitumor activity. *J Med Chem.* **2007**, *50*, 2767-2778.

25. Felip, E.; Barlesi, F.; Besse, B.; Chu, Q.; Gandhi, L.; Kim, S. W.; Carcereny, E.; Sequist, L. V.; Brunsvig, P.; Chouaid, C.; Smit, E. F.; Groen, H. J. M.; Kim, D. W.; Park, K.; Avsar, E.; Szpakowski, S.; Akimov, M.; Garon, E. B. Phase 2 Study of the HSP-90 Inhibitor AUY922 in Previously Treated and Molecularly Defined Patients with Advanced Non-Small Cell Lung Cancer. *J Thorac Oncol.* **2018**, *13*, 576-584.
26. Goldman, J. W.; Raju, R. N.; Gordon, G. A.; El-Hariry, I.; Teofilivici, F.; Vukovic, V. M.; Bradley, R.; Karol, M. D.; Chen, Y.; Guo, W.; Inoue, T.; Rosen, L. S. A first in human, safety, pharmacokinetics, and clinical activity phase I study of once weekly administration of the Hsp90 inhibitor ganetespib (STA-9090) in patients with solid malignancies. *BMC Cancer* **2013**, *13*, 152.
27. a) Shapiro, G. I; Kwak, E.; Dezube, B. J.; Yule, M.; Ayrton, J.; Lyons, J.; Mahadevan, D. First-in-human phase I dose escalation study of a second-generation non-ansamycin HSP90 inhibitor, AT13387, in patients with advanced solid tumors. *Clin Cancer Res.* **2015**, *21*, 87-97.
    b) https://www.uchealth.com/research/clinical-study/?id=49734fb4-053e-4d17-9dd7-64cc4382fa23 (accessed 28th August, 2019).
28. Modi, S.; Saura, C.; Henderson, C.; Lin, N. U.; Mahtani, R.; Goddard, J.; Rodenas, E. Hudis, C.; O'Shaughnessy, J.; Baselga, J. A multicenter trial evaluating retaspimycin HCL (IPI-504) plus trastuzumab in patients with advanced or metastatic HER2-positive breast cancer. *Breast Cancer Res. Treat*. **2013**, *139*, 107-113.

29. Johnson, M. L.; Yu, H. A.; Hart, E. M.; Weitner, B. B.; Rademaker, A. W.; Patel, J. D.; Kris, M. G.; Riely, G. J. Phase I/II study of HSP90 inhibitor AUY922 and erlotinib for EGFR-mutant lung cancer with acquired resistance to epidermal growth factor receptor tyrosine kinase inhibitors. *J. Clin. Oncol.* **2015**, *33*, 1666-1673.

30. Socinski, M. A.; Goldman, J.; El-Hariry, I.; Koczywas, M.; Vukovic, V..; Horn, L.; Paschold, E.; Salgia, R.; West, H.; Sequist, L. V. ; Bonomi, P.; Brahmer. J.; Chen, L. C.; Sandler, A.; Belani, C. P.; Webb, T.; Harper, H.; Huberman, M.; Ramalingam, S.; Wong, K. K.; Teofilovici, F.; Guo, W.; Shapiro, G. I. A multicenter phase II study of ganetespib monotherapy in patients with genotypically defined advanced non-small cell lung cancer. *Clin. Cancer Res.* **2013,** *19*, 3068 - 3077.

31. Wayne, N.; Mishra, P; Bolon, D. N. Hsp90 and client protein maturation, *Meth. Mol. Biol.* **2011,** *787*, 33 - 44.

32. Whitesell, L.; Lindquist, S. L. HSP90 and the chaperoning of cancer. *Nat. Rev. Cancer* **2005**, *5*, 761 - 772.

33. Whitesell, L.; Mimnaugh, E. G.; De Costa, B.; Myers, C. E.; Neckers, L. M. Inhibition of heat shock protein HSP90-pp60v-src heteroprotein complex formation bybenzoquinone ansamycins: essential role for stress proteins in oncogenictransformation. *Proc. Natl. Acad. Sci. U. S. A.*, **1994,** *91*, 8324 - 8328.

34. (a) Kim, S. H.; Kang, J. G.; Kim, C. S.; Ihm, S. H.; Choi, M. G.; Yoo, H. J.; Lee, S. The heat shock protein 90 inhibitor SNX5422 has a synergistic activity with histone deacetylase inhibitors in induction of death of anaplastic thyroid carcinoma cells. *Endocrine* **2016**, *51*, 274 -282. (b) Rao, R.; Fiskus, W.; Yang, Y.; Lee, P.; Joshi, R.; Fernandez, P.; Mandawat, A.; Atadja, P.; Bradner, J.E.; Bhalla, K. HDAC6 inhibition enhances 17-AA Gemediated

abrogation of hsp90 chaperone function in human leukemia cells. *Blood* **2008**, *112*, 1886 - 1893. c) Rahmani, M, Yu, C.; Dai, Y.; Reese, E.; Ahmed, W.; Dent, P.; Grant, S. Coadministration of the heat shock protein 90 antagonist 17-allylamino-17-demethoxygeldanamycin with suberoylanilide hydroxamic acid or sodium butyrate synergistically induces apoptosis in human leukemia cells. *Canc. Res.* **2003**, *63*, 8420 - 8427. d) George, P.; Bali, P.; Annavarapu, S.; Scuto, A.; Fiskus, W.; Guo, F.; Sigua, C.; Sondarva, G.; Moscinski, L.; Atadja, P. Combination of the histone deacetylase inhibitor LBH589 and the hsp90 inhibitor 17-AAG is highly active against human CML-BC cells and AML cells with activating mutation of FLT-3. *Blood* **2005**, *105*, 1768 - 1776.

35. Deskin, B.; Shan, B.; Lasky, J. Targeting The Hdac6/hsp90 Axis To Destabilize The Notch1 Receptor In Non-Small Cell Lung Cancer. *Am. J. Respir. Crit. Care Med.* **2016**, *193*, A2374.
36. Ojha, R.; Huang, H. L.; HuangFu, W. C.; Wu, Y. W.; Nepali, K.; Lai, M, J.; Su, C. J.; Sung, T. Y.; Chen, Y. L.; Pan, S. L.; Liou, J. P. 1-Aroylindoline-hydroxamic acids as anticancer agents, inhibitors of HSP90 and HDAC. *Eur. J. Med. Chem.* **2018**, *150*, 667 – 677.
37. (a) Lai, M. J.; Huang, H. L.; Pan, S. L.; Liu, Y. M.; Peng, C. Y.; Lee, H. Y.; Yeh, T. K.; Huang, P. H.; Teng, C. M.; Chen, C. S.; Chuang, H. Y, Liou, J. P. Synthesis and biological evaluationof 1-arylsulfonyl-5-(N-hydroxyacrylamide)indoles as potent histone deacetylaseinhibitors with antitumor activity in vivo. *J. Med. Chem.* **2012**, *55*, 3777 - 3791. (b) Lee, H. Y.; Yang, C. R.; Lai, M. J, Huang, H. L, Hsieh, Y. L.; Liu, Y. M.; Yeh, T. K.; Li, Y. H.; Mehndiratta, S.; Teng, C. M.; Liou, J. P. 1-Arylsulfonyl-5-(N-hydroxyacrylamide) indolines histone deacetylase inhibitors are potent cytokine release suppressors. *Chembiochem.* **2013**, *14*, 1248 - 1254. (c) Huang, H. L.; Lee, H. Y.; Tsai, A. C.; Peng, C. Y.; Ai, L. M. J.; Wang, J. C.; Pan, S. L.; Teng, C. M.; Liou, J. P. Anticancer activity of MPT0E028, a novel

potent histone deacetylaseinhibitor, in human colorectal cancer HCT116 cells in vitro and in vivo. *PLoS One* **2012**, *7*, 43645. (d) Lee, H. Y.; Tsai, A. C.; Chen, M. C.; Shen, P. J.; Cheng, Y. C.; Uo, K. C. C.; Pan, S. L.; Liu, Y. M.; Liu, J. F.; Yeh, T. K.; Wang, J. C.; Chang, C. Y.; Chang, J. Y.; Liou, J. P. Azaindolylsulfonamides,with a more selective inhibitory effect on histone deacetylase 6 activity, exhibit antitumor activity in colorectal cancer HCT116 cells. *J. Med. Chem.* **2014**, *57*, 4009 - 4022. (e) Liu, Y. M.; Lee, H. Y.; Chen, C. H.; Lee, C. H.; Wang, L. T.; Pan, S. L.; Lai, M. J.; Yeh, T. K.; Liou, J. P. 1-Arylsulfonyl-5-(N-hydroxyacrylamide)tetrahydroquinolines aspotent histone deacetylase inhibitors suppressing the growth of prostatecancer cells. *Eur. J. Med. Chem.* **2015**, *89*, 320 - 330.

38. a) Proia, D.A.; Bates, R.C. Ganetespib and HSP90: translating preclinical hypotheses into clinical promise. *Canc. Res.* **2014**, *74*, 1294-1300. b) a) Johnson, M.L.; Yu, H.A.; Hart, E.M.; Weitner, B.B.; Rademaker, A.W.; Patel, J.D.; Kris, M.G.; Riely, G.J. Phase I/II study of HSP90 inhibitor AUY922 and erlotinib for EGFR-mutant lung cancer with acquired resistance to epidermal growth factor receptor tyrosine kinase inhibitors. *J. Clin. Oncol.* **2015**, *33*, 1666–1673. b) Rathi, R.N.; Ramalingam, S.R. Throwing More Cold Water on Heat Shock Protein 90Inhibitors in NSCLC. *J. Thor. Onc.* **2018**, *13*, 473-474. c) Bhat, R.; Tummalapalli, S.R, Rotella, D.P. Progress in the discovery and development of heat shock protein 90 (Hsp90) inhibitors, *J. Med. Chem.* **2014**, *21*, 8718-28.

39. Nepali, K.; Lin, M.H.; Chao, M.W.; Peng, S.J.; Hsu, K.C.; Lin, T.E.; Chen, M.C.; Lai, M.J.; Pan, S.L.; Liou, J.P. Amide-tethered quinoline-resorcinol conjugates as a new class of HSP90 inhibitors suppressing the growth of prostate cancer cells. *Bioorganic chemistry*, **2019**, *91*, 103119.

40. Chan KC, Ting CM, Chan PS, Lo MC, Lo KW, Curry JE, Smyth T, Lee AW, Ng WT, Tsao GS, Wong RN, Lung ML, Mak NK. A novel Hsp90 inhibitor AT13387 induces senescence in EBV-positive nasopharyngeal carcinoma cells and suppresses tumor formation. *Mol Cancer.* **2013**, *12*, 128.

41. Watson, P. J.; Fairall, L.; Santos, G. M.; Schwabe, J. W. Structure of HDAC3 bound to co-repressor and inositol tetraphosphate. *Nature.* **2012**, 481, 335-340.

42. (a) Falkenberg, K. J.; Johnstone, R. W. Histone deacetylases and their inhibitors in cancer, neurological diseases and immune disorder. *Nat Rev Drug Discov.* **2014**, 13, 673-91. (b) Srinivasarao, M.; Galliford, C. V.; Low, P.S. Principles in the design of ligand-targeted cancer therapeutics and imaging agents. *Nat Rev Drug Discov.* **2015,** 14, 203-19.

43. Vogerl, K.; Ong, N.; Senger, J.; Herp, D.; Schmidtkunz, K.; Marek, M.; Muller, M.; Bartel, K.; Shaik, T.B.; Porter, N.J.; Robaa, D.; Christianson, D.W.; Romier, C.; Sippl, W.; Jung, M.; Bracher, F. Synthesis and Biological Investigation of Phenothiazine-Based Benzhydroxamic Acids as Selective Histone Deacetylase 6 Inhibitors. *J. Med. Chem.* **2019**, *62*, 1138-1166.

44. Porter, N.J.; Mahendran, A.; Breslow, R.; Christianson, D.W. Unusual zinc-binding mode of HDAC6-selective hydroxamate inhibitors. *Proc Natl Acad Sci U S A* **2017**, *114*, 13459-13464.

45. Barril, X.; Beswick, M. C.; Collier, A.; Drysdale, M. J.; Dymock, B. W.; Fink, A .; Grant, K.; Howes, R.; Jordan, A. M .; Massey, A.; Surgenor, A.; Wayne, J.; Workman, P.; Wright, L. 4-Amino derivatives of the Hsp90 inhibitor CCT018159. *Bioorg. Med. Chem. Lett.* **2006**, 16, 2543-2548.

46. Zhang, L.; Zhang, J.; Jiang, Q. X.; Zhang, L.; Song, W. G. Zinc binding groups for histone deacetylase inhibitors. *J. Enzym. Inhib. Med. Chem.* **2018**, 33, 714-721.

47. Osinska, I.; Popko, K. & Demkow U. Perforin: an important player in immune response. *Cent Eur. J. Immunol.* **2014**, *39*, 109-115.

48. a) Lanitis, E., Dangaj, D., Irving, M. & Coukos, G. Mechanisms regulating T-cell infiltration and activity in solid tumors. *Ann. Oncol.* **2017**, *28*, xii18-xii32 b) Jiang, X.; Wang, J.; Deng, X.; Xiong, F.; Ge, J.; Xiang, B.; Wu, X.; Ma, J.; Zhou, M.; Li, X.; Li, Y.; Li, G.; Xiong, W.; Guo, C.; Zeng, Z. Role of the tumor microenvironment in PD-L1/PD-1 mediated tumor immune escape. *Mol. Canc.* **2019**, *18*, 10 c) Spranger, S.; Spaapen, R. M.; Zha, Y.; Williams, J.; Meng, Y.; Ha, T. T.; Gajewski, T. F. Up-regulation of PD-L1, IDO, and T (regs) in the melanoma tumor microenvironment is driven by CD8(+) T cells. *Sci. Transl. Med.* **2013**, *5*, 200ra116. d) He, J.; Hu, Y.; Hu, M. & Li, B. Development of PD-1/PD-L1 Pathway in Tumor Immune Microenvironment and Treatment for Non-Small Cell Lung Cancer. *Sci. Rep.* **2015**, *5*, 13110.

49. LeadIT B. http://www. biosolveit. de/LeadIT. *accessed 12th Jan.* **2011**.

50. Berman, H.M.; Westbrook, J.; Feng, Z.; Gilliland, G.; Bhat, T.N.; Weissig, H.; Shindyalov, I.N.; Bourne, P.E.The Protein Data Bank. *Nucleic Acids Res.* **2000**, 28, 235-242.

Figure Captions

Figure 1. (A) Structures of HDAC and HSP90 inhibitors; (B) Designed dual HDAC/HSP90 inhibitors.

Figure 2. Western blot analysis of histone H3 and α-tubulin acetylation after treatment with 17 and SAHA.

Figure 3. Compound 17 triggered degradation of multiple HSP90 client proteins in a concentration- and time-dependent manner.

Figure 4. Compound 17 induces accumulation of a sub-G1 phase population and significant cell apoptosis in H1975 cells.

Figure 5. Confirmation of docking protocol.

Figure 6. Interaction analysis of active compounds in HSP90.

Figure 7. Interaction analysis of active compounds in HDAC6.

Figure 8. HDAC structural differences leads to HDAC6 selectivity.

Figure 9. Antitumor efficacy of compound 17 alone and in combination with Afatinib in NSCLC H1975 xenograft model.

Figure 10. Compound 17 downregulated PD-L1 expression in INF-γ treated H1975 lung cancer cells.

Table 1. Antiproliferative activity of compounds **10 - 18** against human lung cancer cell lines

Compounds	**A549**	**H1975**
	GI_{50} (μM ± SD)[a]	
10	0.37 ± 0.30	0.13 ± 0.05
11	0.83 ± 0.25	0.39 ± 0.08
12	> 10	> 10
13	0.87 ± 0.11	1.64 ± 0.49
14	2.22 ± 0.33	0.68 ± 0.22
15	2.92 ± 0.18	4.34 ± 0.84
16	2.35 ± 0.14	1.07 ± 0.29
17	0.76 ± 0.13	0.52 ± 0.20
18	2.74 ± 0.38	0.32 ± 0.11
1	1.02 ± 0.15	0.98 ± 0.31
6	0.33 ± 0.02	0.20 ± 0.03

[a]SD: standard deviation, all experiments were independently performed at least three times

Table 2. Inhibition of HeLa nuclear extract HDAC Activity and HSP90 chaperone protein by compounds **10-18**

Compound	**HSP90a**	**HeLa HDAC**
	IC_{50} (nM ± SD)[a]	
10	66.0 ± 5.7	> 1000
11	123.1 ± 33.9	> 1000
12	135.6 ± 13.2	> 1000
13	108.7 ± 17.0	> 1000
14	43.9 ± 1.6	521.4 ± 67.1
15	43.9 ± 3.5	168.3 ± 31.5
16	42.2 ± 3.2	198.9 ± 50.8
17	46.8 ± 6.4	388.8 ± 20.9
18	103.5 ± 10.3	> 1000
1	> 1000	99.4 ± 17.7
6	65.7 ± 1.6	> 1000

[a]SD: standard deviation, all experiments were independently performed at least three times

Table 3: HDAC isoform inhibitory activity of compounds **10 - 18**

Compds (selectivity ratio)[b]	IC_{50} (nM)[a]			
	HDAC1	HDAC3	HDAC6	HDAC8
10	> 10000 (> 300)	9851 (296)	33.3 (-)	420 (12.6)
11			>10000	7319
12	7431 (108)	4411 (64.3)	68.6 (-)	
13	6885 (20.8)	2811 (8.5)	330 (-)	7415 (22.5)
14	3814 (404)	2209 (234)	9.44 (-)	2011 (213)
15	554 (250)	388 (175)	2.21 (-)	1510 (683)
16	1075 (507)	494 (233)	2.12 (-)	> 10000 (> 4716)
17	1878 (434)	1312 (303)	4.32 (-)	3720 (861)
18	3150 (10.4)	3991 (13.2)	303 (-)	675 (2.2)
Trichostatin A	6.96 (2.7)	10.4 (4)	2.60 (-)	820 (315)

[a]All compounds were dissolved in DMSO and tested in at least 10-dose IC_{50} mode with 3-fold serial dilution starting at 10 μM. IC_{50} values displayed the result of a single experiment. These assays were conducted by the Reaction Biology Corporation, Malvern, PA. [b]Selectivity ratio = selectivity ratio of HDAC subtypes over HDAC6. *Empty cells indicate no inhibition or compound activity that could not be fitted to an IC_{50} curve.

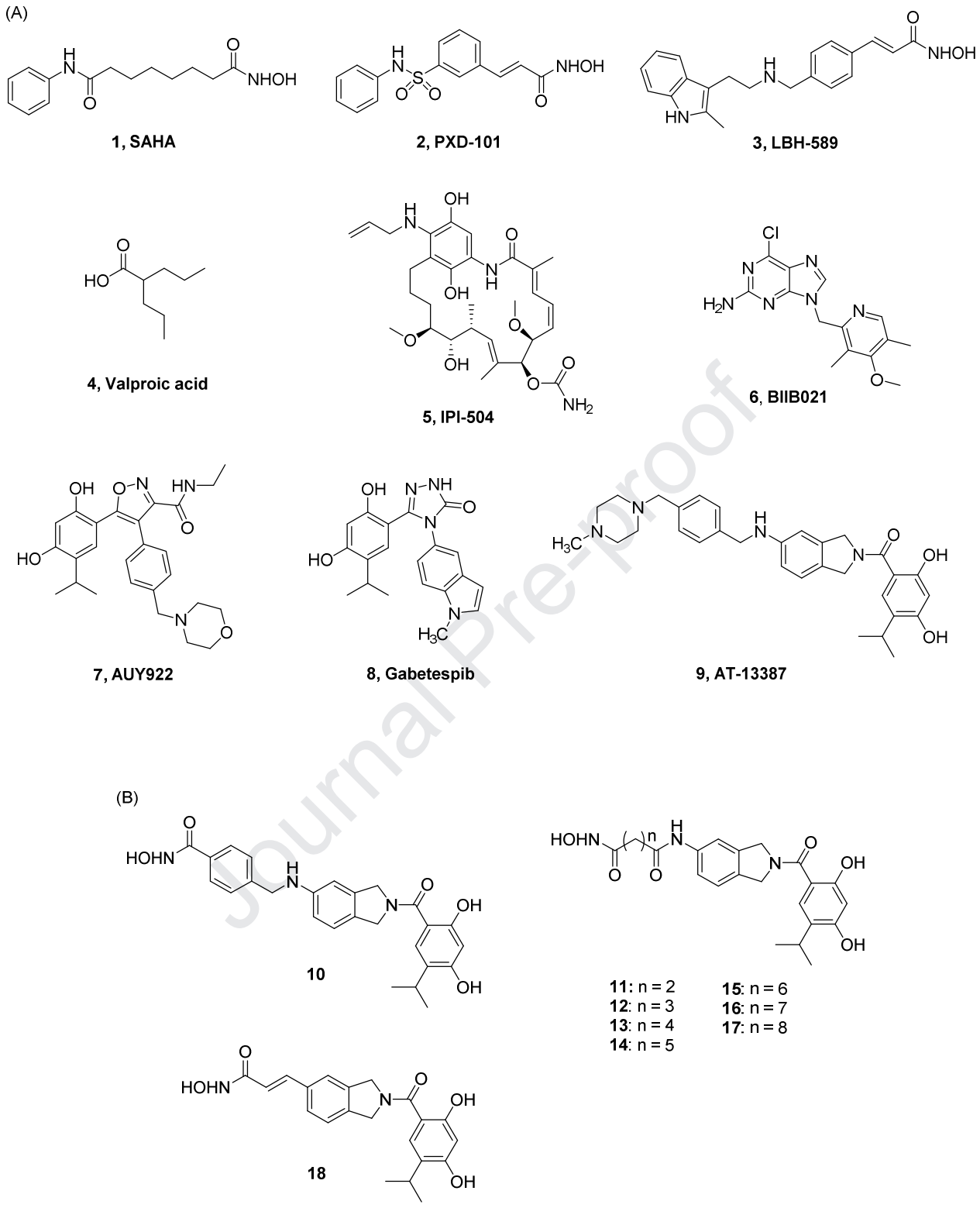

Figure 1. (A) Structures of HDAC and HSP90 inhibitors; (B) Designed dual HDAC/HSP90 inhibitors

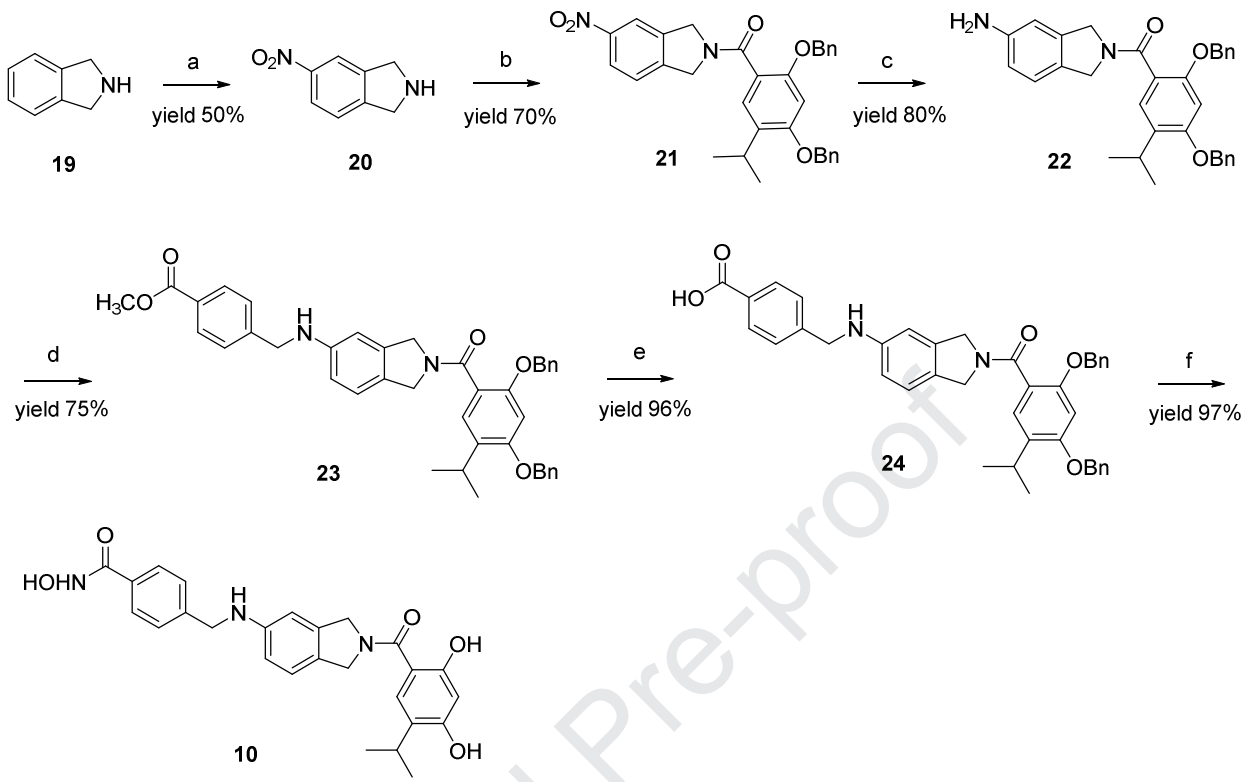

Scheme 1. Reagents and conditions: (a) HNO_3, H_2SO_4, DCM, 0 °C to rt; (b) 2,4-bis(benzyloxy)-5-isopropylbenzoic acid, EDC, HOBt, DIPEA, DCM, rt; (c) Fe, NH_4Cl, EtOH: H_2O: 4:1, reflux; (d) methyl 4-formylbenzoate, $NaCNBH_3$, EtOH, rt; (e) 1 M LiOH(aq), *p*-dioxane, 40°C; (f) i. $NH_2OBn.HCl$, EDC, HOBt, DIPEA, DMF, rt; ii. BCl_3 (1M in heptane), DCM, 0°C.

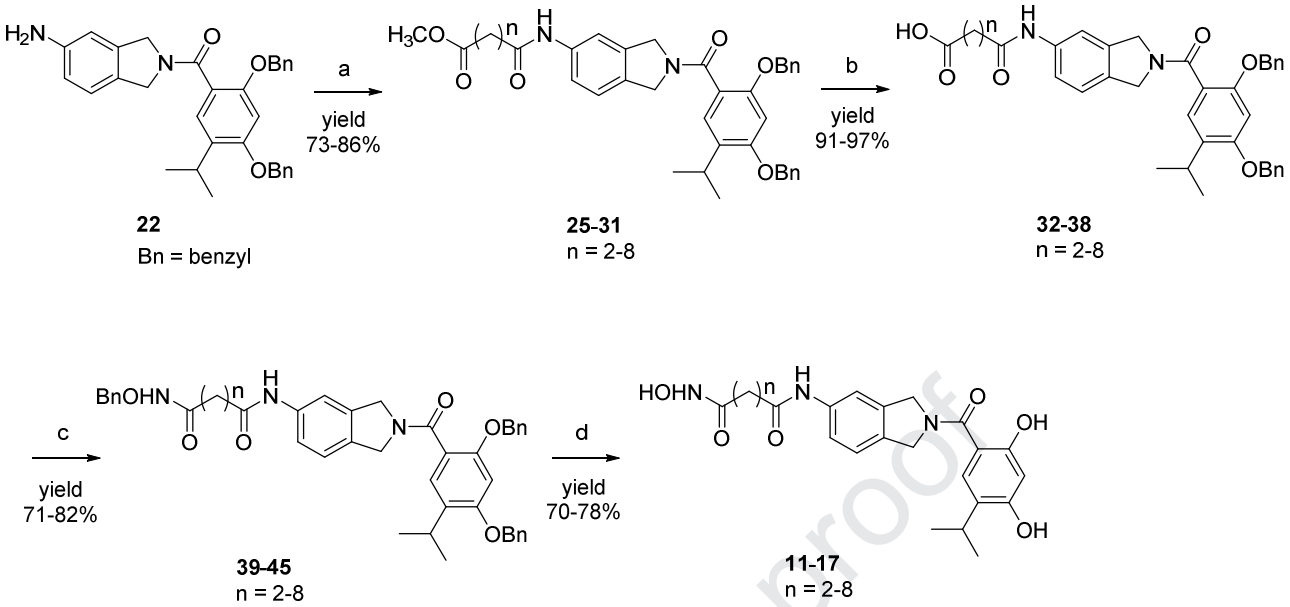

Scheme 2. Reagents and conditions: (a) alkoxy oxoalkanoic acid, EDC, HOBt, DIPEA, DMF, rt; (b) LiOH (1 M, aq), dioxane, 40 °C; (c) $NH_2OBn.HCl$, EDC, HOBt, DIPEA, DMF, rt; (d) Pd/C, H_2, CH_3OH, rt.

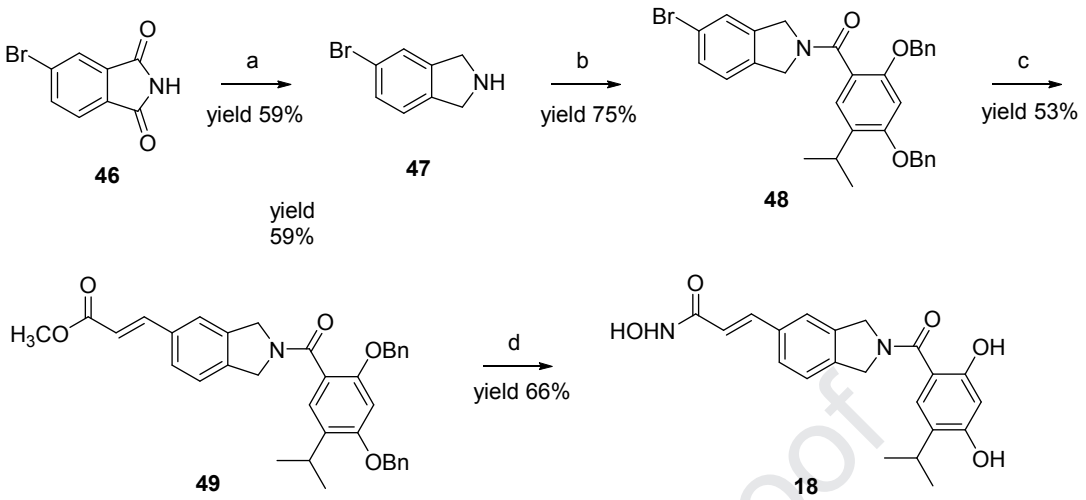

Scheme 3. Reagents and conditions: (a) $NaBH_4$, BH_3-THF, THF, reflux; (b) 2,4-dihydroxy-5-isopropylbenzoic acid, EDC, HOBt, DIPEA, DCM, rt; (c) methyl acrylate, $Pd(OAC)_2$, $(C_6H_5)_3P$, TEA, DMF, 100 °C, rt; (d) i. LiOH, dioxane, rt ii. NH_2OBn, EDC, HOBt, DIPEA, DMF, rt iii. BCl_3, DCM, 0 °C.

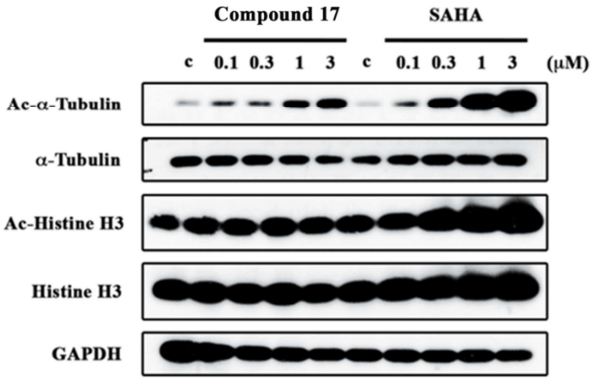

Figure 2. Western blot analysis of histone H3 and α-tubulin acetylation after treatment with **17** and SAHA. H1975 cells were treated with **17** or SAHA at the indicated concentrations for 24 h. The protein levels of acetyl-histone H3, acetyl-α-tubulin and GAPDH were determined by Western blot analysis.

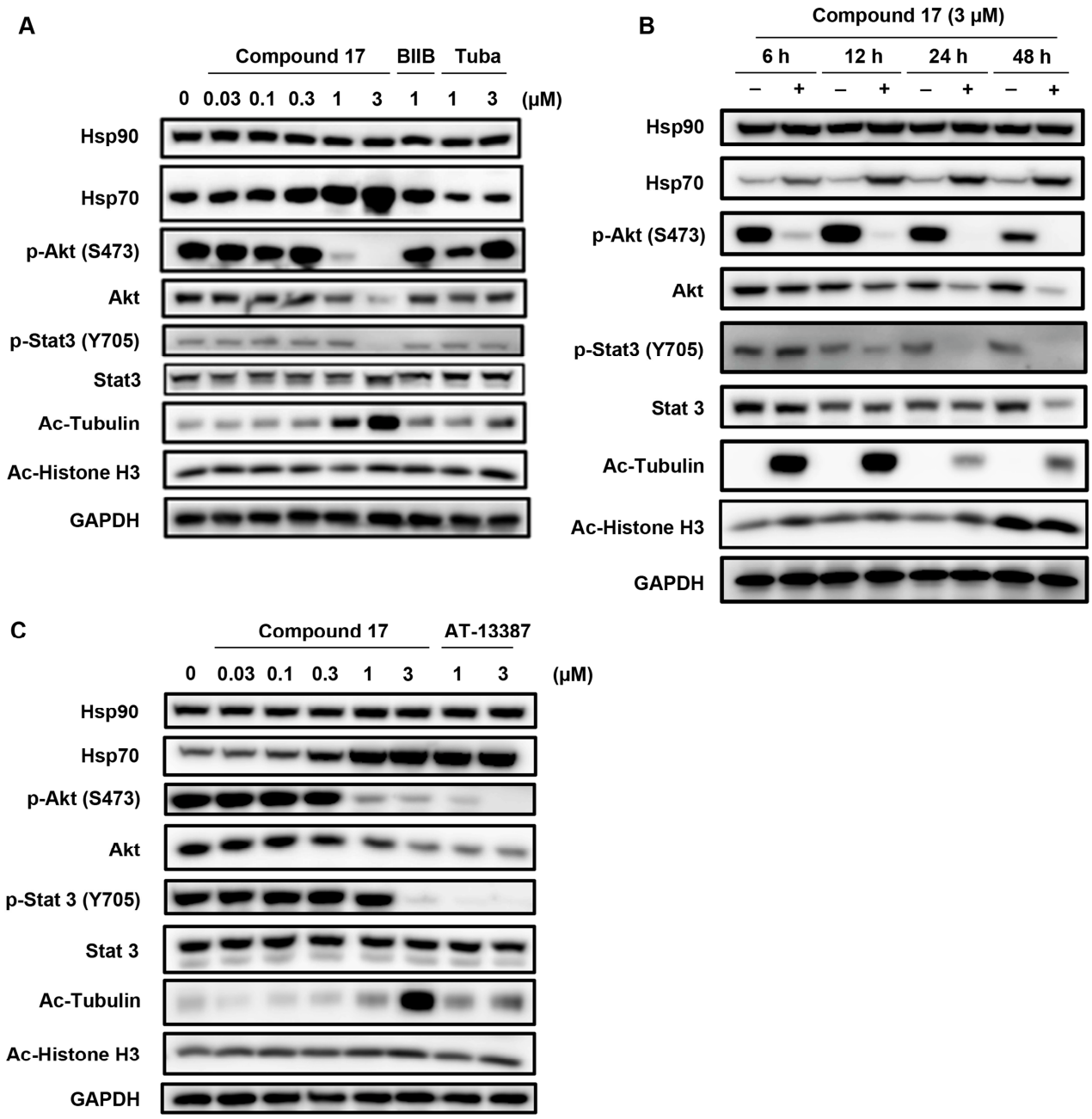

Figure 3. Compound **17** triggered degradation of multiple HSP90 client proteins in a concentration- and time-dependent manner. A) H1975 cells were treated with DMSO or 0.03-3 μM of test compounds (**17**, BIIB021, and Tubastatin A) for 24 h. Cells were harvested and subjected to Western blot analysis for the detection of various HSP90 client proteins. B) H1975 cells were treated with 3 μM of **17** for indicated times. C) H1975 cells were treated DMSO or indicated concentrations of test compounds (**17** and AT-13387) for 24 h. Whole cell lysates were collected, and each protein expression was detected by immunoblotting. GAPDH was used as the internal control. BIIB (BIIB021); Tuba (Tubastatin A).

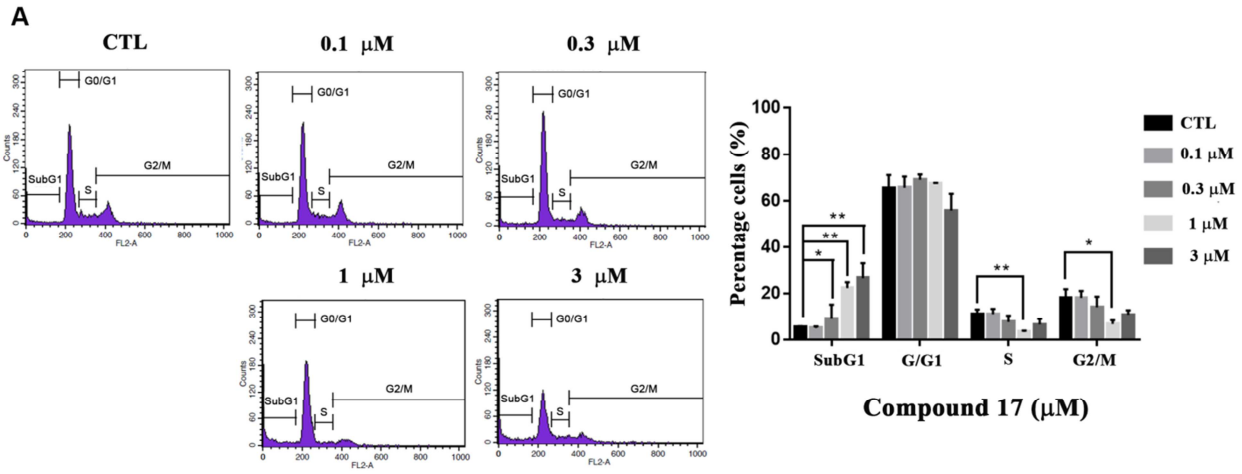

B

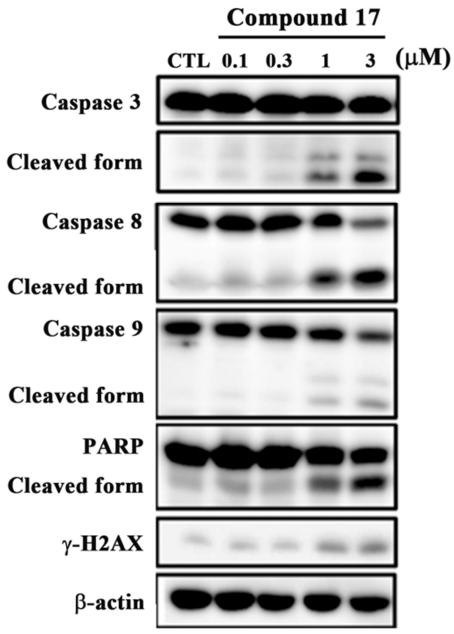

Figure 4. Compound **17** induces accumulation of a sub-G1 phase population and significant cell apoptosis in H1975 cells. A) Compound **17** induces sub-G1 phase cells accumulation after 48 h treatment (left panel), and the bar graph shows a statistical analysis of the results of cell cycle distribution by the student's *t*-test (right panel). Results are from a single representative experiment that was carried out n = 3 times. B) Compound **17** induces cell apoptotic death in H1975 cells. Cells were cultured with indicated concentrations of Compound **17** for 48 h and cell lysates were detected by indicated antibodies.

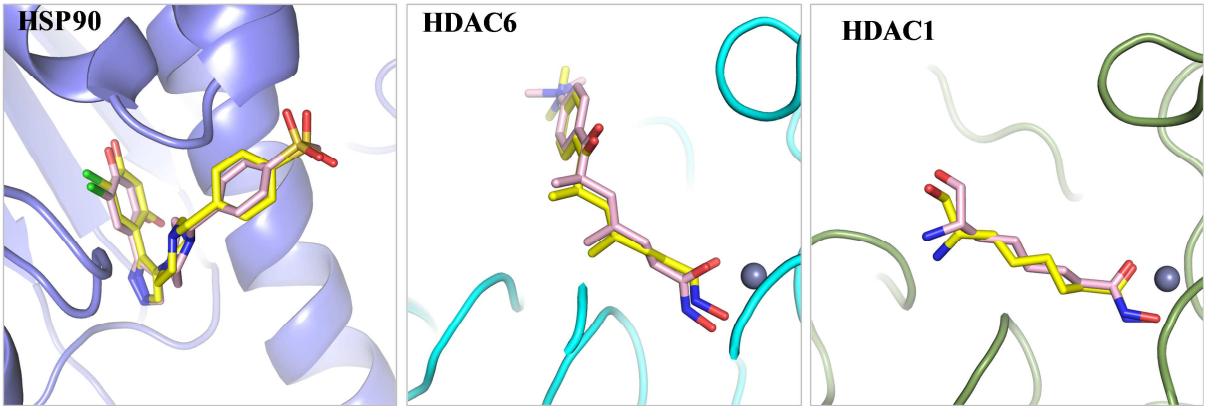

Figure 5. **Confirmation of docking protocol.** The docking protocol was confirmed by redocking the co-crystallized ligand. The docked ligands (red) produced a pose similar those of the co-crystallized ligand (yellow). Protein targets are labeled as shown - HSP90 (PDB ID: 2CCU), HDAC6 (PDB ID: 5EDU), HDAC1 (PDB ID: 5ICN)

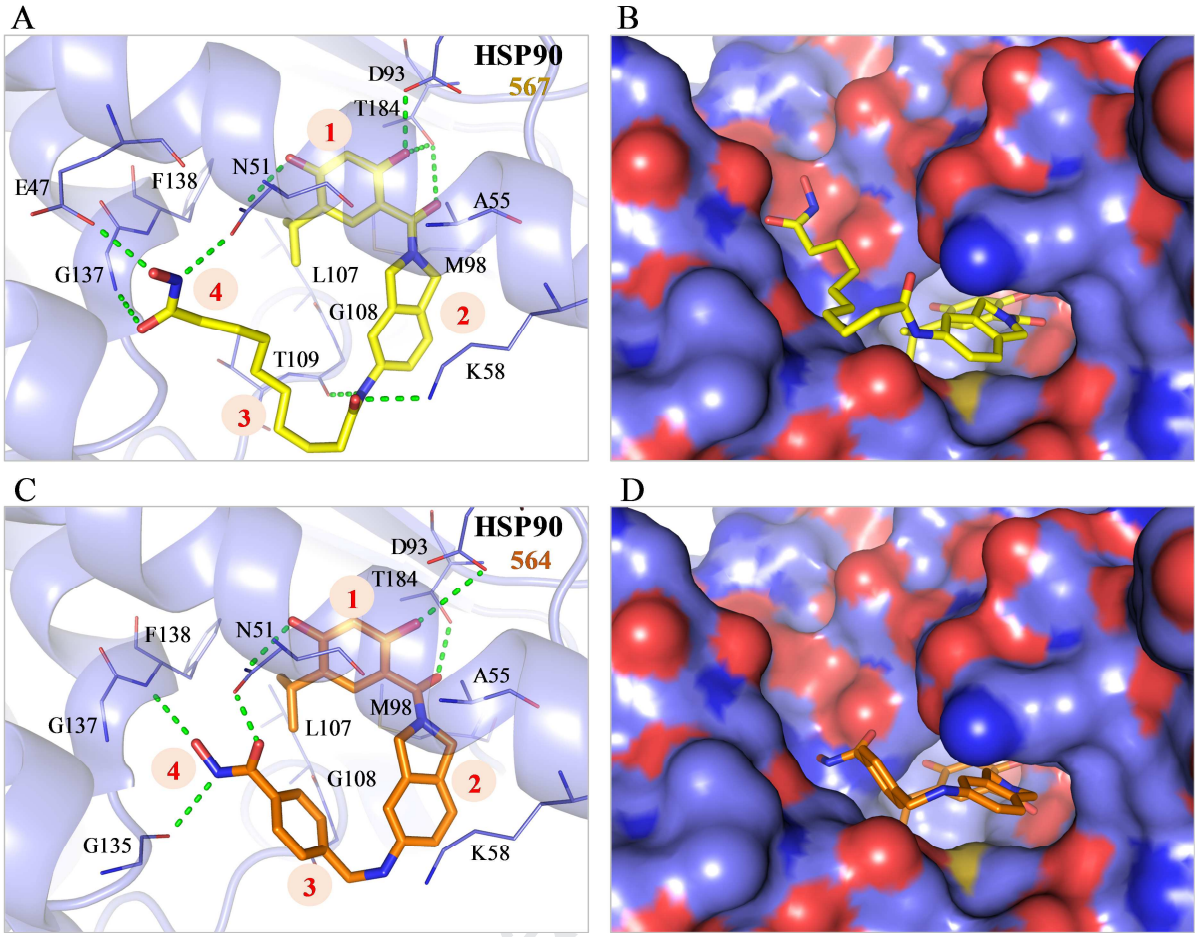

Figure 6. **Interaction analysis of active compounds in HSP90** (PDB ID: 2CCU)**.** (A) The docking pose of compound **17** (yellow) in the HSP90 binding site (purple). (B) The surface model shows that compound **17** enters the binding site unencumbered. (C) The docking pose of compound **10** (orange) in HSP90 binding site (purple). (D) The docking surface model does not show any obstruction to compound **10** in the binding site. The compound groups are labeled as shown. Hydrogen bonds are represented as green lines.

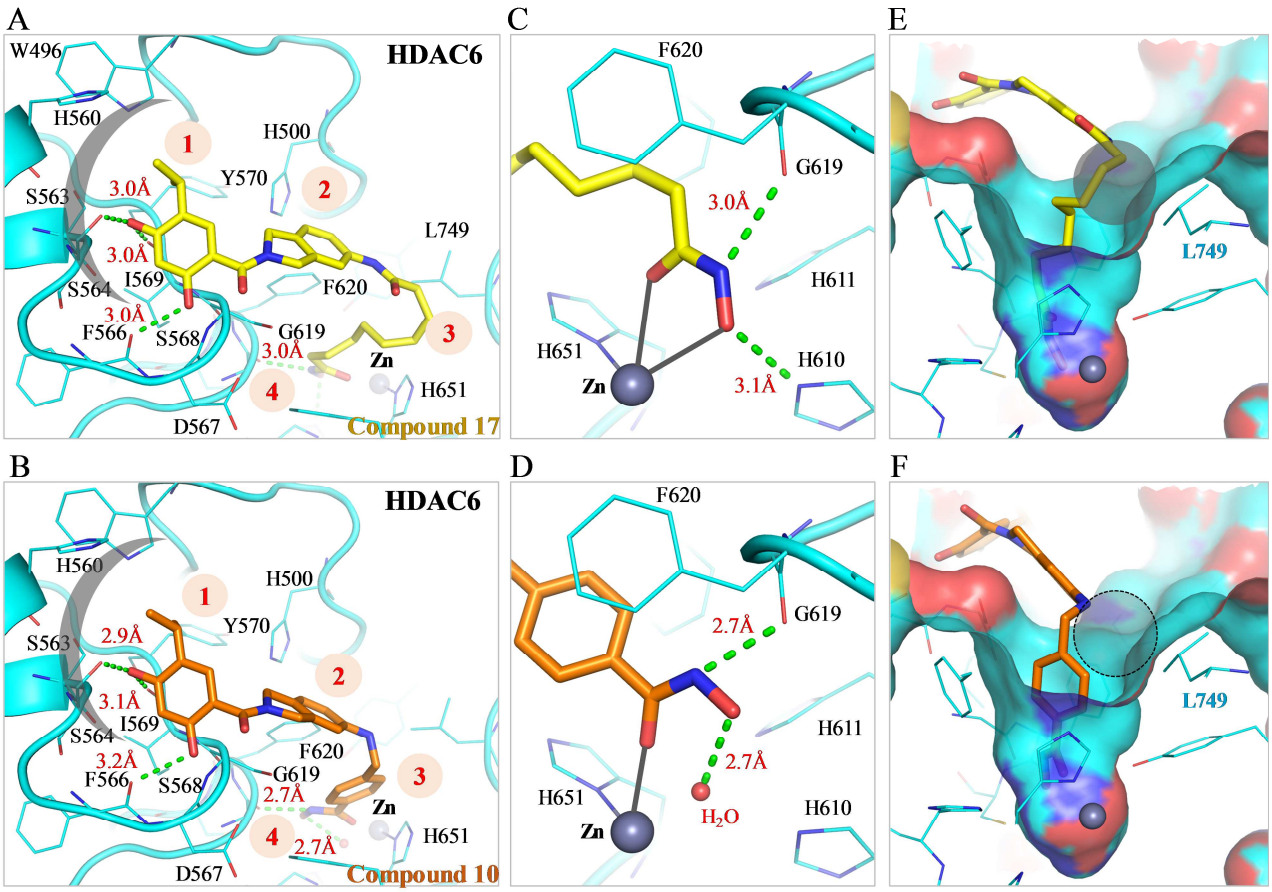

Figure 7. Interaction analysis of active compounds in HDAC6. The docking poses of (A) compound **17** (yellow) and (B) compound **10** (orange) in HDAC6 (blue). The compound groups are labeled as shown. (C-D) the ZBG of active compounds coordinate to the Zn^{2+} and forms hydrogen bonds with nearby residues. The HDAC6 surface model shows (E) compound **17** and (F) compound **10** interactions along the catalytic site. The dash circle represents different interactions between the active compound linkers and HDAC6. Hydrogen bonds are shown represented as dashed green lines and the distance in red.

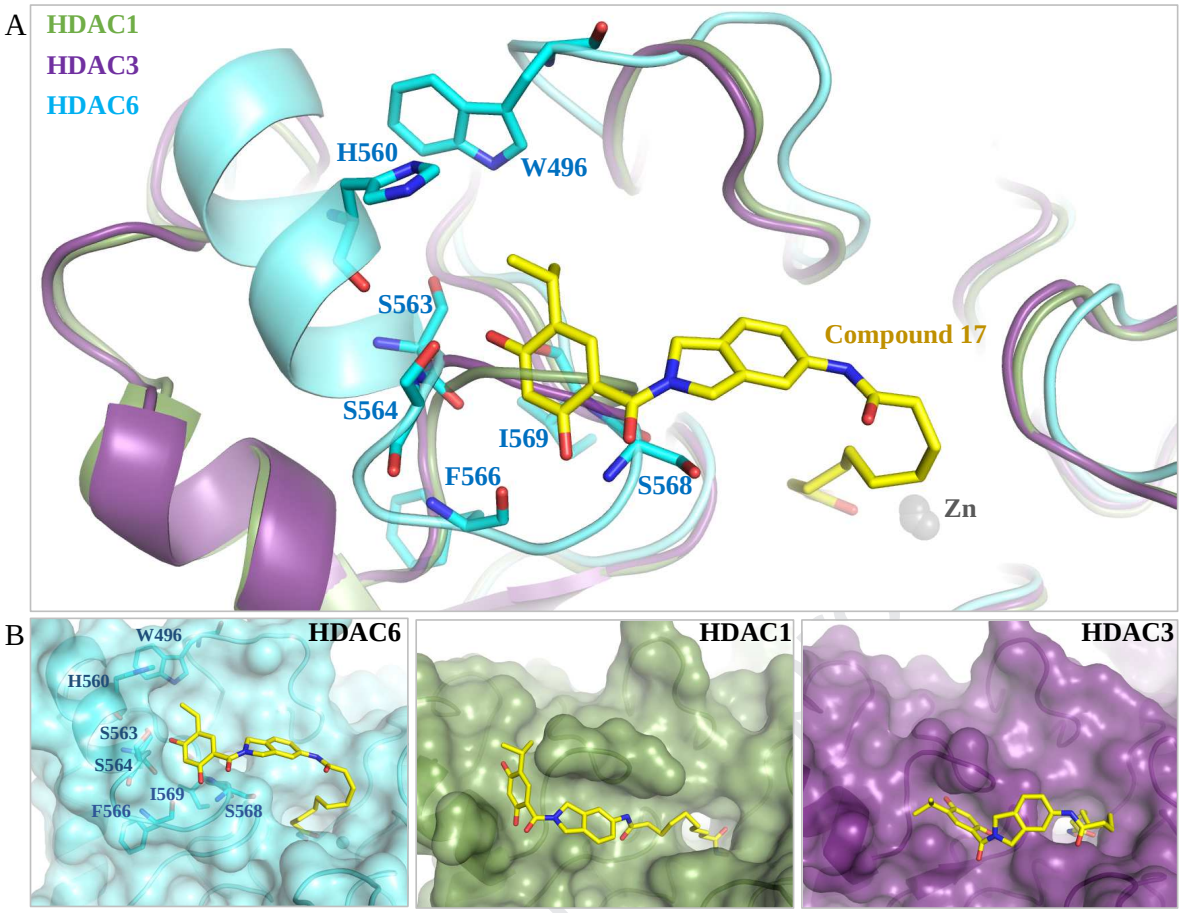

Figure 8. HDAC structural differences leads to HDAC6 selectivity. (A) The docked pose of compound **17** (yellow) in HDA6 (blue) are superimposed with HDAC1 (green) and HDAC3 (purple). (B) The surface model of compound **17** docked in HDAC6, HDAC1 and HDAC3. A specific pocket for the cap group is observed in HDAC6.

A

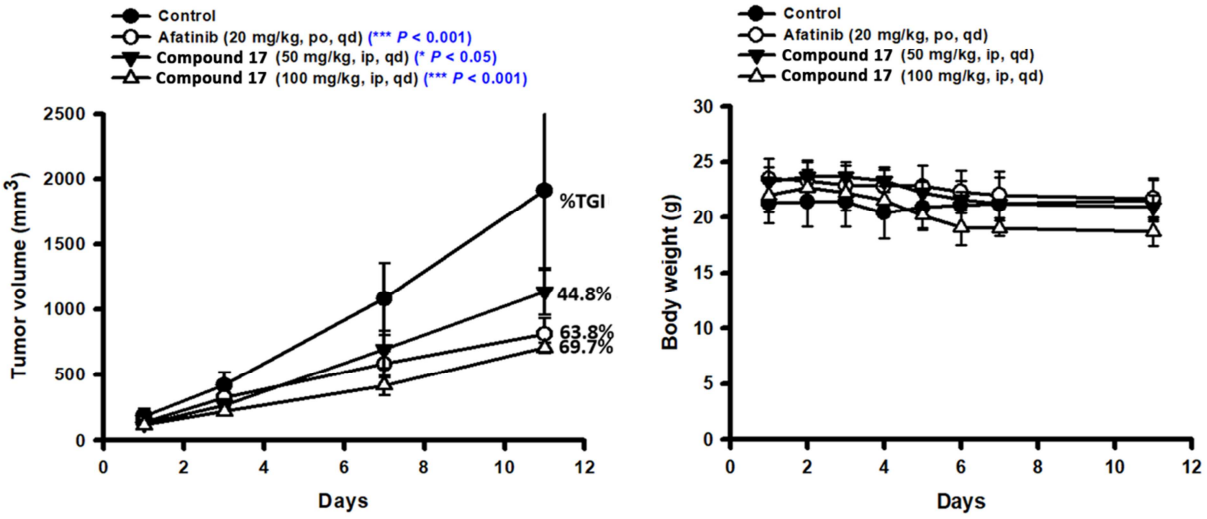

B

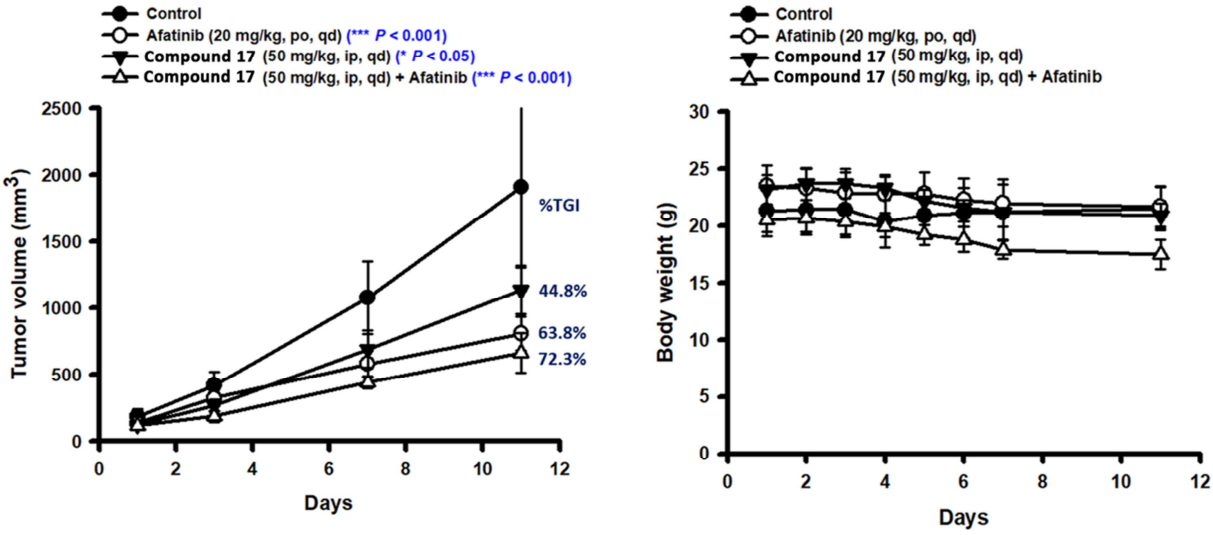

Figure 9. Antitumor efficacy of compound **17** alone and in combination with Afatinib in NSCLC H1975 xenograft model. A) Tumor volume (left) and body weight changes (right) of different of treatment groups. B) Enhanced antitumor efficacy of compound **17** in combination with afatinib (left). Toxicity assessment in different treatment groups was measured by body weight (right). Tumor growth was calculated by the mean tumor volume (mm^3) ± SE and calculated as % tumor growth inhibition (%TGI). Tumor volume was determined using caliper measurements and was calculated as the product of 1/2 × length × $width^2$ as described in Materials and Methods.

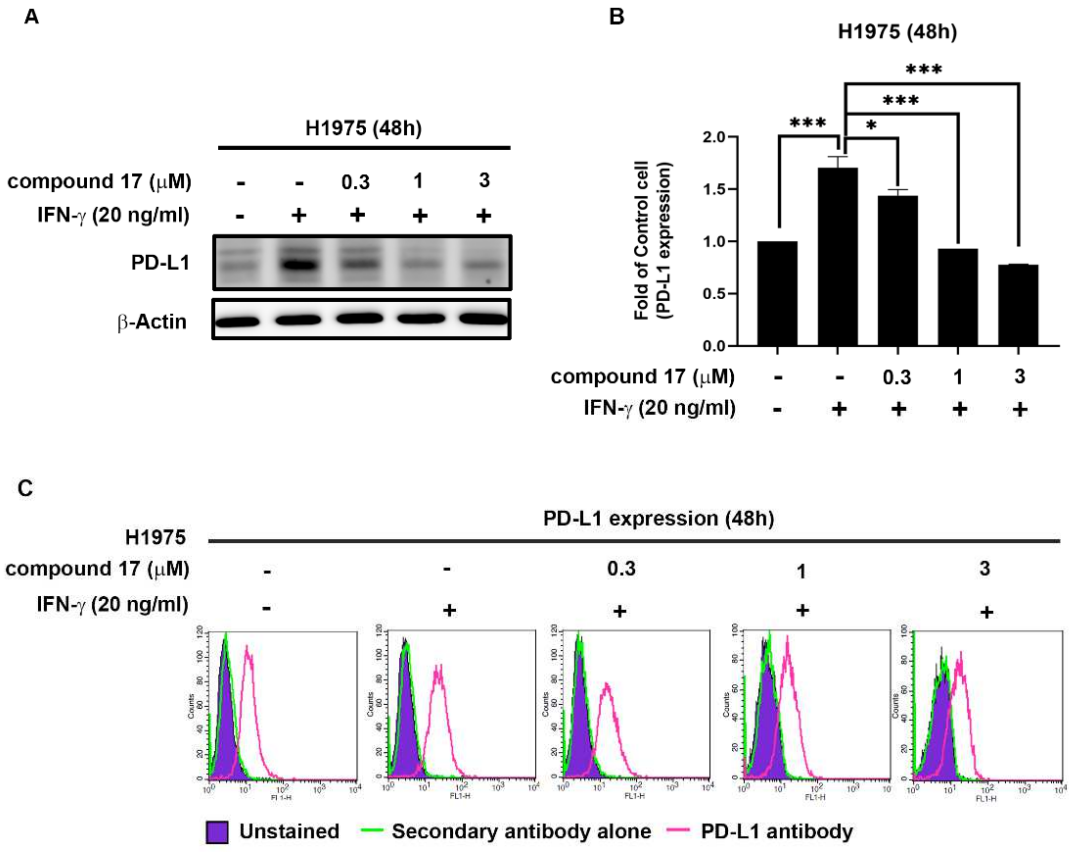

Figure 10. Compound 17 downregulated PD-L1 expression in INF-γ treated H1975 lung cancer cells. (A) Cells were treated with the IFN- γ alone (20 ng/ml) or in combination with compound **17** at the indicated concentrations for 48 h, and total cell lysates were analyzed by Western blotting with PD-L1 antibody. (B and C) Cell where treated with IFN-γ alone (20 ng/ml) or in combination with Compound **17** at the indicated concentrations for 48 h, and analyzed by flow cytometry. **(B)** The MFI of treated cells is presented relative as the MFI of non-treated cells. The data are presented as mean ± S.D. obtained from three independent experiments. ***$P < 0.001$, *$P < 0.05$ compared with the INF-γ alone group.

Research highlights

1. 1-Aroylisoindoline-hydroxamic acids as dual HDAC6/HSP90 inhibitors have been synthesized.
2. Compound **17** displays potent inhibition of HDAC6 isoform and HSP90a inhibition.
3. Compound **17** induced suppression of tumor growth both in monotherapy as well as the combination therapy with afatinib in human H1975 xenografts.
4. Compound **17** downregulated PD-L1 expression in INF-γ treated H1975 lung cancer cells.
5. Compound **17** in combination with T cell immunotherapy might be worth investigating for treatment of cancer.

Declaration of interests

☒ The authors declare that they have no known competing financial interests or personal relationships that could have appeared to influence the work reported in this paper.

☐The authors declare the following financial interests/personal relationships which may be considered as potential competing interests: